Quaternary Science Reviews 215 (2019) 144–159

Contents lists available at ScienceDirect

Quaternary Science Reviews

journal homepage: www.elsevier.com/locate/quascirev

Late Holocene hydroclimate variability in Costa Rica: Signature of the terminal classic drought and the Medieval Climate Anomaly in the northern tropical Americas

Jiaying Wu [a, *, 1], David F. Porinchu [a], Sally P. Horn [b]

[a] Department of Geography, University of Georgia, Athens, GA, 30602, USA
[b] Department of Geography, University of Tennessee, Knoxville, TN, 37996, USA

ARTICLE INFO

Article history:
Received 7 February 2019
Received in revised form
25 April 2019
Accepted 26 April 2019

Keywords:
Chironomids
Lago morrenas 3C
Laguna zoncho
Paleoclimate
Thermal reconstruction
Drought
Climatic mechanism
Tropical americas
Tropical north atlantic
Global change

ABSTRACT

In the northern tropical Americas (Neotropics), notable hydrological variability has been documented in multi-proxy paleoclimate records between ~600 and 1200 CE. This interval generally overlaps with the Maya Terminal Classic Drought (TCD: ~770–1100 CE) and the Medieval Climate Anomaly (MCA: ~950–1250 CE). There is, however, limited paleoclimate data that provide reliable estimates of terrestrial thermal variability in southern Central America during this time. In this study, we present chironomid-based temperature reconstructions, developed from sediment cores from two lakes: (1) Lago Morrenas 3C, a high-elevation glacial lake located on the crest of the Atlantic slope of the Cordillera Talamanca, Costa Rica, and (2) Laguna Zoncho, a mid-elevation lake located on the Pacific slope in southern Costa Rica. Distinctive shifts in the chironomid assemblages occurred at both sites between ~610 and 1230 CE. These changes are inferred to reflect an ~600-year interval characterized by depressed mean annual temperatures at Lago Morrenas 3C and dry conditions and lake level decline at Laguna Zoncho. Taken together, the multi-proxy paleoclimate records from these two lakes, including stable carbon isotope ($\delta^{13}C$) and charcoal data, suggest that middle elevations on the Pacific slope and high elevations on the Atlantic slope of Costa Rica experienced sustained drought, and possible cooling coeval with the TCD-MCA interval. The timing of hydroclimate variability in these records provides support for the hypothesis that cooling and drought in the northern tropical Americas during the TCD and early MCA were linked to thermal changes in the tropical North Atlantic.

1. Introduction

During the past two decades, a substantial and increasing number of paleoclimate and paleoenvironmental studies have documented the existence of notable climate variability during medieval times, generally spanning from ~600 to 1200 CE (Mann et al., 2008, 2009; Graham et al., 2011; Douglas et al., 2016). A global synthesis of high-resolution paleoclimate records indicates that the interval between ~950 and 1250 CE was characterized by anomalously high surface air temperatures in the middle and high latitudes of the Northern Hemisphere (Mann et al., 2008, 2009). This interval, broadly known as the Medieval Climate Anomaly (MCA: ~950–1250 CE) (Mann et al., 2008, 2009), was likely marked by extended and persistent La Niña-like conditions, with depressed sea surface temperatures (SSTs) and reduced precipitation in the eastern tropical Pacific (Seager et al., 2007; Graham et al., 2011).

In the Yucatan Peninsula, where many of the high-resolution reconstructions of hydroclimate variability have been developed for the northern tropical Americas, the MCA interval largely overlaps with an event that is regionally known as the Maya Terminal Classic Drought (TCD) (Hodell et al., 1995; Curtis et al., 1996; Hodell et al., 2001, 2005; Rosenmeier et al., 2002; Webster et al., 2007; Medina-Elizalde et al., 2010; Hodell et al., 2012; Kennett et al., 2012; Wahl et al., 2013; Douglas et al., 2015). The TCD is characterized by a series of moderate to severe drought episodes between ~770 and 1100 CE (Hodell et al., 2005). These droughts have long been considered as a crucial trigger for the socioeconomic "collapse" of Classic Maya civilization at ~1000 CE (Weiss and Bradley, 2001; Kennett et al., 2012; Medina-Elizalde and Rohling, 2012; Douglas

* Corresponding author.
E-mail address: jiaywu@fiu.edu (J. Wu).
[1] Present address: Southeast Research Center, Department of Earth and Environment, Florida International University, Miami, FL 33199.

https://doi.org/10.1016/j.quascirev.2019.04.023
0277-3791/

et al., 2016), although it is likely that the "collapse" of the Maya was a complex process that involved a multitude of human-environment interactions (Aimers and Hodell, 2011; Luzzadder-Beach et al., 2012; Turner and Sabloff, 2012; Douglas et al., 2016). Studies from elsewhere in the northern tropical Americas, including southern Central America (Lachniet et al., 2004), northern South America (Moy et al., 2002; Haug et al., 2003) and the circum-Caribbean (Lane et al., 2011a and 2014), also document an interval characterized by repeated drought episodes between ~770 and 1250 CE, broadly corresponding with the MCA. The hydrological fluctuations that characterize the interval between ~770 and 1250 CE in the northern tropical Americas, however, appear to be spatially and temporally variable. A paucity of high-resolution records documenting thermal variability during the TCD and MCA in the northern tropical Americas limits our ability to decipher the mechanism(s) that drove the anomalous hydroclimate variability in this region between ~ 770 and 1250 CE.

Costa Rica, located in southern Central America, has been the location of numerous paleoenvironmental studies and reconstructions during recent decades. Paleoenvironmental research in Costa Rica has focused on glacial history (Orvis and Horn, 2000; Lachniet and Seltzer, 2002; Potter et al., 2019) and on documenting changes in vegetation, fire regimes, hydrology, climate, and anthropogenic activity during the late Quaternary (Horn and Sanford, 1992; Horn, 1993; League and Horn, 2000; Clement and Horn, 2001; Lachniet et al., 2004; Anchukaitis and Horn, 2005; Kennedy and Horn, 2008; Lane et al., 2011a; Lane and Horn, 2013; Taylor et al., 2013(a,b); 2015; Wu et al., 2017; Wu et al., 2019; Wu and Porinchu, under review). Highly resolved records of late Holocene paleoenvironmental change in Costa Rica, specifically studies focused on reconstructing thermal variability, remain limited. We recently developed a quantitative reconstruction of late Holocene mean annual air temperature (MAAT) using sub-fossil chironomid assemblages preserved in a sediment core recovered from Laguna Zoncho, in southern Costa Rica (Wu et al., 2017). During the TCD and the MCA, sub-fossil chironomid remains were sparse or absent in the Laguna Zoncho sediment core, hindering the development of a quantitative reconstruction of thermal conditions during that interval (Wu et al., 2017). We attribute the rarity of chironomid remains to greatly reduced lake levels between ~730 and 1110 CE, reflecting decreased effective moisture, potentially in response to a regional manifestation of the TCD.

To address the lack of high-resolution thermal records spanning the late Holocene in Costa Rica, we present a sub-decadal to multi-decadal-scale thermal reconstruction extending back to ~300 CE for this region. The reconstruction of thermal conditions was produced by analyzing the subfossil chironomid remains preserved in a short sediment core extracted from a high-elevation glacial lake, Lago Morrenas 3C (MOR3C; Horn et al., 2005), in Chirripo National Park (NP) in the Cordillera de Talamanca of south-central Costa Rica. The chironomid-based thermal reconstruction from MOR3C, together with reconstructions of fire regime and vegetation dynamics at the same site (Wu and Porinchu, under review), are compared to the multi-proxy reconstruction developed for Laguna Zoncho (Wu et al., 2017), a mid-elevation lake located in the southern Pacific region of Costa Rica, near the border with Panama. Our objective was to characterize the variability of hydroclimate across a 2300-m elevation gradient in southern Central America during the late Holocene, with specific attention paid to the TCD-MCA interval. Additionally, these records are compared with existing paleoclimate and paleoenvironmental studies from the tropical Americas to assess the linkages between proposed driver(s) of hydroclimate variability and paleoenvironmental change in Costa Rica during the TCD-MCA interval from 770 to 1250 CE.

1.1. Study site

Lago Morrenas 3C (MOR3C) (9°29′44″ N, 83°29′06″ W; 3492 m a.s.l.; Horn et al., 2005) is a small (0.9 ha) glacial lake with maximum depth of 2 m, located in the Valle de las Morrenas in Chirripó National Park (NP), Costa Rica (Fig. 1; Table 1). The bedrock underlying Morrenas 3C consists of crystalline granitoid intrusives of the Miocene-age Talamancan intrusive series (Orvis and Horn, 2000), with younger lavas and interbedded tuffs, agglomerates, and tuffites making up the adjacent ridge of Cerro Laguna (Wunsche al., 1999). Lago Morrenas 3C is surrounded by páramo vegetation composed of diverse assemblages of evergreen shrubs, grasses, and perennial herbs of largely Andean origin (Luteyn, 1999; Kappelle and Horn, 2016). The páramo ecosystem in Chirripó NP extends from 3300 to 3819 m a.s.l. and is dominated by the dwarf bamboo *Chusquea subtessellata*, which covers up to 60% of the páramo in Costa Rica (Kappelle, 1991; Kappelle and Horn, 2016). While the dominant bamboo and most herbaceous plants in the páramo are C_3 plants, three species of *Muhlenbergia*, a native C_4 grass, occur in the páramo (Lane et al., 2011a), along with some possible C_4 sedges. *M. flabellata*, the most common species of *Muhlenbergia*, is abundant at the margin of Lago Morrenas 3C. *Muhlenbergia* can tolerate low temperatures (Schwarz and Redmann, 1988; Sage et al., 1999) and is widely distributed in cold environments, including the boreal forest of Canada and in alpine settings in the Rocky Mountains (Sage et al., 1999). Under drier conditions, C_3 herbaceous plants in the páramo could become more C_4-like in their carbon isotopic signatures, resulting in more positive $\delta^{13}C$ values in soils and sediments when effective moisture is low at the site (Diefendorf et al., 2010; Kohn, 2010).

Long-term meteorological data are not available for Chirripó NP, but records from the Cerro Páramo station (3,466 m a.s.l.; 9°33′36″ N, 83°45′11″W), which is located ~30 km west of Cerro Chirripó in the Buenavista páramo, have been regarded as broadly representative (Horn, 1993). The mean annual air temperature (MAAT) and mean annual precipitation at Cerro Páramo between 1971 and 2000 were 8.5 °C and 2581 mm, respectively (Lane et al., 2011a). The precipitation record from the Cerro Páramo station documents distinct dry and wet seasons, with 89% of the precipitation falling during the wet season, which occurs between May and November (Kappelle and Horn, 2016). While this seasonal pattern also typifies the Chirripó páramo, Kappelle and Horn (2016) recently estimated that much of the Chirripó páramo may receive less precipitation, perhaps only 1000–2000 mm annually. Monthly rainfall from September 2015 to June 2017, measured using a weather sensor kit installed at a height of 2 m at the Base Crestones shelter (3,400 m a.s.l., ~4.8 km SSW of Lago Morrenas 3C; Esquivel-Hernández et al., 2018), is consistent with an annual total in this range.

The Chirripó páramo straddles the crest of the Cordillera de Talamanca, which constitutes the divide between the Atlantic and Pacific slopes in southern Costa Rica. The páramo experiences dry conditions during the boreal winter, similar to the precipitation regime that characterizes the lower Pacific slope (Coen, 1983). The dry and wet seasons on the Chirripó massif and Pacific slope of Costa Rica are strongly influenced by the seasonal migration of the Intertropical Convergence Zone (ITCZ) (Lane et al., 2011a), which reaches its southernmost position during the boreal winter (Coen, 1983). Other important influences on the climate of the Chirripó massif include the trade winds, the trade wind inversion, cold continental air outbreaks, and Caribbean cyclones (Coen, 1983; Waylen et al., 1996; Esquivel-Hernández et al., 2018). Strong convective activity over Cerro Chirripó is observed during the late boreal summer when the ITCZ moves to its northernmost position and there is an onshore flow of Pacific moisture (Maldonado et al., 2018). During the boreal winter, convective activity weakens, and

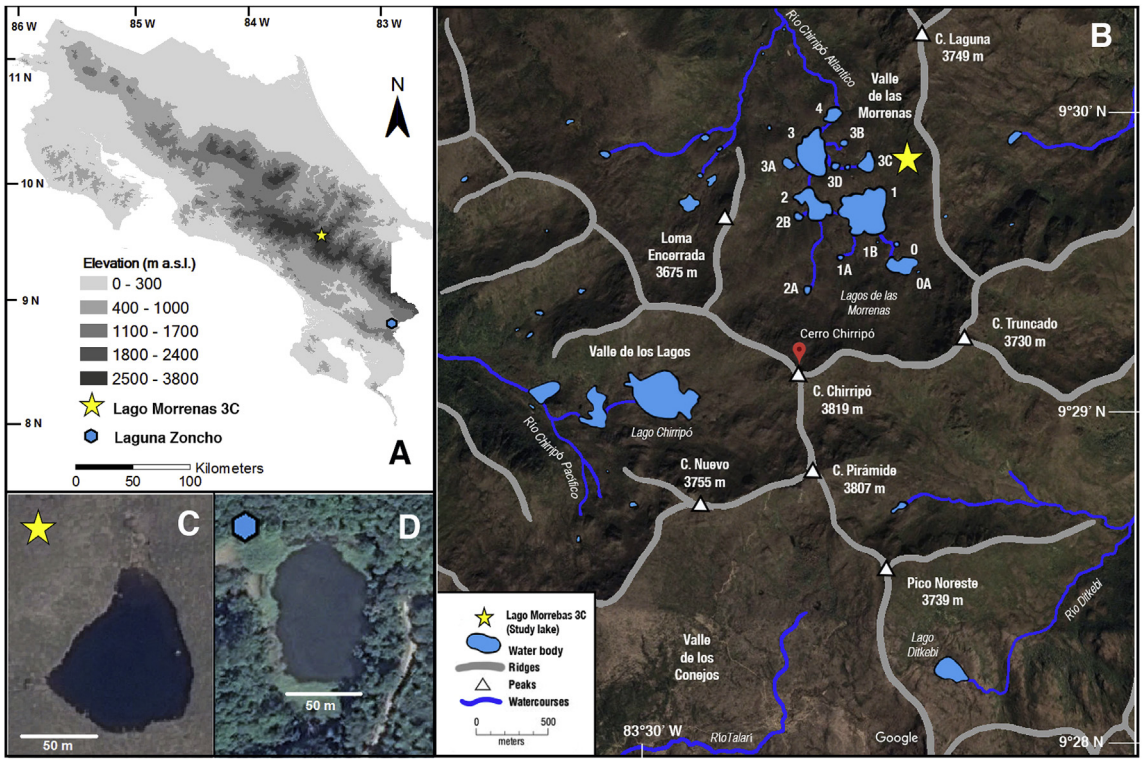

Fig. 1. A) Location of Lago Morrenas 3C and Laguna Zoncho, Costa Rica; **B)** Location of Lago Morrenas 3C, Chirripó National Park, Costa Rica (base maps originate from Orvis and Horn, 2000 and cropped from Google Earth Image ©2018 CNES/Airbus and Image ©2018 DigitalGlobe, modified by Jiaying Wu); **C)** Aerial photo of Lago Morrenas 3C; and **D)** Aerial photo of Laguna Zoncho.

Table 1
Geographic and limnological information for Lago Morrenas 3C and Laguna Zoncho, Costa Rica. Zoncho data are from Horn and Haberyan et al. (1995).

Lake Name	Date Visited (yyyy.mm)	Latitude N. Longitude W.	Elevation m a.s.l.	Depth (m)	Length (m)	Width (m)	Area (ha)	Temperature (°C)	DO (%)	DO (mgl-1)	SPC (mScm-1)	Conductivity (uScm-1)	pH
Lago Morrenas 3C	2014.07	9°29′44″,83°29′06″	3492	2.0	110	80	0.90	8.8	64.4	4.9	0.003	2.3	7.18
Lago Zoncho	1997.07	8°48′44″, 82°57′38″	1190	2.6	105	62	0.55	24.6		7.1		16	7.4

the height of the northeast trade wind inversion decreases, often falling below the elevation of the high peaks (Lane et al., 2011a). Thus, whereas the Atlantic slope below the summit páramo region experiences high rainfall through the year because of the persistent onshore flow of Caribbean moisture carried by the northeast trade winds, with especially heavy precipitation at mid-elevations (Coen, 1983), the páramo on the upper Atlantic slope, where Morrenas 3C is located, experiences lower rainfall during the boreal winter. Moisture from the Caribbean may somewhat temper the dry season for plants, by increasing humidity along the crest of the Cordillera Talamanca relative to lower elevations on the Pacific slope. But intervals of cloud-free weather associated with the northeast trade wind inversion during the dry season can lower humidity sufficiently to support fires (Horn, 1993; Horn and Kappelle, 2009).

2. Methods

2.1. Fieldwork

In July 2014, a 40.5-cm sediment core was recovered from the center of Lago MOR3C using a DeGrand maxi-corer, which is a modified gravity corer (Glew, 1991). The stratigraphy of MOR3C core was described from the bottom to the top of the core in the field before sectioning. Notable changes in color occurred with depth. The sediment was characterized by a mixture of organic matter and a low amount of algae/fecal pellet material between 40.5 cm and 35 cm, resulting in dark brown to black sediment in the base portion of the core. An interval with a high concentration of algae/fecal pellets, observed at 34 cm, resulted in yellow to light-brown sediment. The sediment between 33 and 22 cm was light-brown due to the continuous presence of relatively high amounts of algae/fecal pellets. The amount of algae/fecal pellets rapidly increased again at 20 cm, peaking at ~21 cm, resulting in sediment colored yellow to light-brown. Algae/fecal pellets were still present, but at a reduced concentration, between 21 cm and 17 cm, making the sediment appear light-brown to brown in color. The sediment between 17 cm and the surface (depth = 0 cm) is characterized by dark-brown to black organic material. The sediment was sectioned at 0.25-cm intervals using a DeGrand vertical sediment extruder in the field, stored in Whirl-pak™ bags, and transported back to the Environmental Change Lab (ECL) in the Department of Geography at the University of Georgia. Sediment samples were stored in a refrigerator at 4 °C in the ECL. Surface water temperature, pH, conductivity and dissolved oxygen were measured during fieldwork (Table 1).

2.2. Chronology

Chronological control for the lake sediment core from MOR3C is based on seven AMS radiocarbon dates obtained on charcoal fragments. Radiocarbon analyses were conducted at the Center for Applied Isotope Studies (CAIS) at the University of Georgia. The radiocarbon dates were converted to calendar years using the IntCal13 calibration curve (CALIB 7.10: calib.org/calib/calib.html; Reimer et al., 2013), with the exception of the "modern" date (pMC = 100.68%, error = 1.03) sampled between 5.75 and 7.5 cm (Table 2). The relative areas of the ± 2σ age ranges and the corresponding median probability ages from CALIB are reported for each radiocarbon date. The age-depth model for the MOR3C core is based on a probability sampling method implemented using Bacon 2.2 with a setting of thick = 2 (Fig. 2; Blaauw and Christen, 2011). The "modern" date was converted into ^{14}C age using post-bomb conversion with a code of "pMC.age ()" in Bacon. The median age of −54 ^{14}C yr BP with an error of ±82 yr was used for the "modern" date in the Bacon age-depth model (postbomb = 2). Two radiocarbon dates (UGAMS#23001, UGAMS#28490; marked in bold in Table 2) were excluded from the final Bacon age-depth model for MOR3C (red dots with calibrated median age labeled in Fig. 2). The date of 990 ^{14}C yr ± 25 yr obtained on the charcoal sample at 10.4 cm is considered anomalously old. This sample likely persisted on the landscape following a fire and was transported to the lake centuries after the fire. The anomalously young date at 14.25 cm, which was based on a sample of charcoal fragments extracted from eight contiguous 0.25-cm intervals, had a low mass (~300 μg) and was likely contaminated by young carbon. The sedimentation rate, which was ~0.020 cm/yr between ~300 and 680 CE, increases to 0.026 cm/yr between 680 and 1040 CE. The sediment accumulation rate, which nearly doubles (~0.049 cm/yr) between 1040 and 1190 CE, rapidly decreases to 0.019 cm/yr between 1190 and 1770 CE. An increase in sedimentation rate to ~0.026 cm/yr characterizes the interval between 1770 CE and the present.

2.3. Chironomids

Chironomids are sensitive to temperature (Porinchu and McDonald, 2003), and the existence of a strong relationship between chironomid distribution and air and water temperature has been documented at many sites in the Northern Hemisphere (e.g. Porinchu et al., 2010; Self et al., 2011; Fortin et al., 2015), including Costa Rica (Wu et al., 2015). Subfossil chironomids preserved in lake sediments recovered from Lago Morrenas 3C are used as a proxy to reconstruct thermal conditions. Sub-fossil chironomids were processed and analyzed following standard procedures (Walker, 2001). A known volume of sediment (3–5 ml) was placed in a beaker with 50 ml of 5% KOH and heated at 50 °C for approximately 30 min. The KOH treatment facilitates the break-up of colloidal matter. The deflocculated sediment was washed through a 95-μm mesh and rinsed using distilled water. The material retained on the mesh was back washed into a beaker. A dissection microscope at 50X and a Bogorov plankton counting tray were used to separate the chironomid head capsules from the sediment matrix. The chironomid head capsules were permanently mounted on slides in

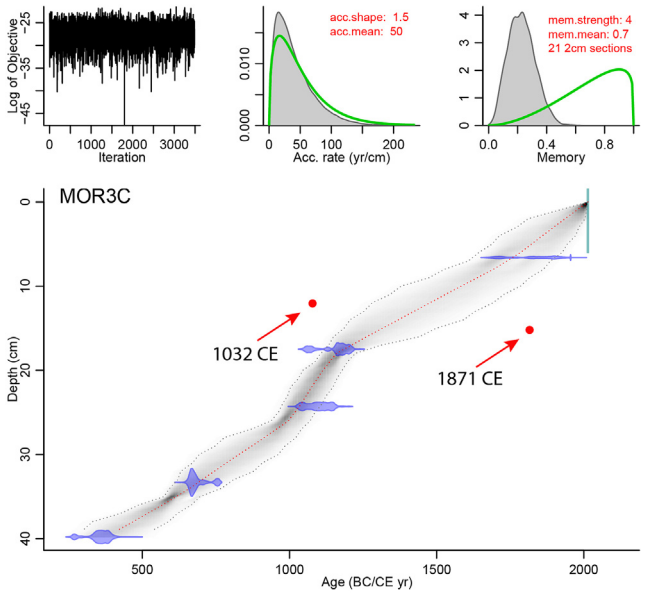

Fig. 2. Age-depth model developed using Bacon 2.2 for the MOR3C core. Two radiocarbon (^{14}C) dates based on charcoal at 10.25 cm and 13.25 cm (the calibrated ages are marked in bold, Table 2.) were not incorporated in the age-depth model (see text for additional details). (For interpretation of the references to color in this figure legend, the reader is referred to the Web version of this article.)

Table 2
AMS radiocarbon dates from MOR3C (dates depicted in bold were not incorporated in the age-depth model; see text for additional details).

Lab code	Core code	Depth in core (cm)	Material	Uncalibrated ^{14}C age (^{14}C yr BP)	±	2σ Age range	Relative area under distribution	Median Probability (CE or cal yr BP)
UGAMS#28489	MOR3C-PT	5.75–7.5	Charcoal	modern	-	1802–1938 CE	0.686	-
						1689-1739 CE	0.252	
						1952–1956 CE	0.036	
						1742-1763 CE	0.026	
UGAMS#23001	**MOR3C-PT**	**10.25–10.5**	**Charcoal**	**990**	**25**	**991-1050 CE**	**0.676**	**1032 CE (918 cal yr BP)**
						1083-1126 CE	**0.259**	
						1136-1151 CE	**0.064**	
UGAMS#28490	**MOR3C-PT**	**13.25–15.25**	**Charcoal**	**60**	**25**	**1875–1918 CE**	**0.566**	**1871 CE (79 cal yr BP)**
						1695-1726 CE	**0.22**	
						1813–1838 CE	**0.158**	
						1842–1853 CE	**0.031**	
						1868–1874 CE	**0.015**	
						1955–1955 CE	**0.01**	
UGAMS#21658	MOR3C-PT	17.25–17.75	Charcoal	880	20	1150-1217 CE	0.773	1169 CE (781 cal yr BP)
						1049-1084 CE	0.192	
						1124-1136 CE	0.035	
UGAMS#23002	MOR3C-PT	24–24.5	Charcoal	940	25	1030-1155 CE	1	1097 CE (853 cal yr BP)
UGAMS#21659	MOR3C-PT	33–33.5	Charcoal	1330	20	652-695 CE	1	671 CE (1279 cal yr BP)
UGAMS#20643	MOR3C-PT	39.5–40	Charcoal	1690	20	326-405 CE	0.926	361 CE (1589 cal yr BP)
						260-279 CE	0.074	

Entellan® for identification. A minimum of 50 chironomid head capsules was identified from each sample (Heiri and Lotter, 2001). Taxonomic identification was conducted at 400X, typically to genus, relying primarily on Wu et al. (2015) and larval keys for Florida and North and South Carolina (Epler, 1995, 2001), with Brooks et al. (2007), Cranston (2010), Eggermont et al. (2008), and Spies et al. (2009) providing additional diagnostic information. Chironomid percentage diagrams, plotted using C2 (Juggins, 2003), were based on the relative abundance of all identifiable chironomid remains. Sub-fossil chironomid remains were analyzed at sub-decadal to multi-decadal resolution, with an average of ~10 yr/sample. Constrained cluster analysis, implemented using the rioja package in R, was used to derive zones for the sub-fossil chironomid stratigraphy (Juggins, 2009; http://cran.r-project.org/package=rioja). Rarefaction analysis was implemented to assess variations in taxonomic richness (Birks and Line, 1992). Shifts in the composition of the sub-fossil chironomid assemblages were assessed using detrended canonical correspondence analysis (DCCA), implemented using CANOCO version 4.0 (Ter Braak and Smilauer, 2002).

3. Results

A total of 14 chironomid taxa were identified in 62 samples in the MOR3C core (Fig. 3). All of the taxa present in MOR3C are found in a modern training set developed using 51 lakes, including MOR3C, in Costa Rica that ranged from 10 to 3520 m a.s.l. (Wu et al., 2015). The sub-fossil chironomid remains, which were well preserved, were present in concentrations between 2.7 and 81 head capsules/ml. The rarefied taxon richness of the chironomid assemblages ranged between 3.0 and 5.9 over the last 1700 years. The greatest change in rarefied taxon richness occurred between ~1250 and 1500 CE, with limited change in richness observed between ~750 and 900 CE. The chironomid stratigraphy is divided into three statistically significant zones (MOR3C–I to MOR3C-III). The chironomid assemblage in the MOR3C core is dominated by four taxa: *Paratanytarsus*, *Tanytarsus* type LU, *Procladius,* and *Psectrocladius;* these four taxa account for 84.6–100% of all the chironomids in the sediment samples in the MOR3C core.

In MOR3C–I (~300–610 CE; 40.5–34.125 cm) the chironomid assemblage is dominated by three taxa, *Paratanytarsus*, *Tanytarsus* type LU, and *Procladius*. *Paratanytarsus* makes up approximately half of the identifiable chironomids in this zone, reaching a core maximum of 65% at ~560 CE. *Tanytarsus* type LU and *Procladius* are ~20% and 15% of the chironomid assemblage, respectively. *Psectrocladius* is also present throughout this zone, albeit with a relatively low abundance, averaging ~5% of the identifiable remains. Two additional chironomid taxa that are intermittently present, *Cricotopus/Orthocladius* and *Limnophyes,* increase in relative abundance toward the end of MOR3C–I. Head capsule concentration fluctuates notably in MOR3C–I, ranging from 15 to 66.8 head capsules/ml (average = 36.9 head capsules/ml). The DCCA scores indicate that the rate of faunal turnover gradually increases through this zone, with rarefied taxon richness range experiencing limited variability (4.1–5.7).

MOR3C-II (610–1230 CE; 34.1–16.25 cm) is characterized by a large increase in the relative abundance of *Psectrocladius* and *Procladius* and an accompanying reduction in the relative abundance of *Paratanytarsus* and *Tanytarsus* type LU. *Psectrocladius* and *Procladius* compose ~25% and 45% of the chironomid assemblages in MOR3C-II, respectively. The relative abundance of *Paratanytarsus* and *Tanytarsus* type LU decreases to ~20% in this zone. Seven additional taxa, *Polypedilum* N type, *Micropsectra contracta* type, *Smittia/Pseudosmittia*, *Cricotopus/Orthocladius, Corynoneura/Thienemanniella*, *Synorthocladius*, and Unknown ii are present in MOR3C-II, albeit at low levels. Of these taxa, only *Cricotopus/Orthocladius*, is present consistently through this zone. Head capsule concentration varies from 10.6 to 81 head capsules/ml (average = 27.1 head capsules/ml) in this zone. DCCA scores increase at the beginning of MOR3C-II, indicating an increase in faunal turnover starting at ~610 CE; they stay generally high during the remainder of this zone. Rarefied taxon richness shows a range (4.0–5.5) in MOR3C-II similar to that in MOR3C–I, with the most stable interval observed between ~750 and 900 cal yr BP.

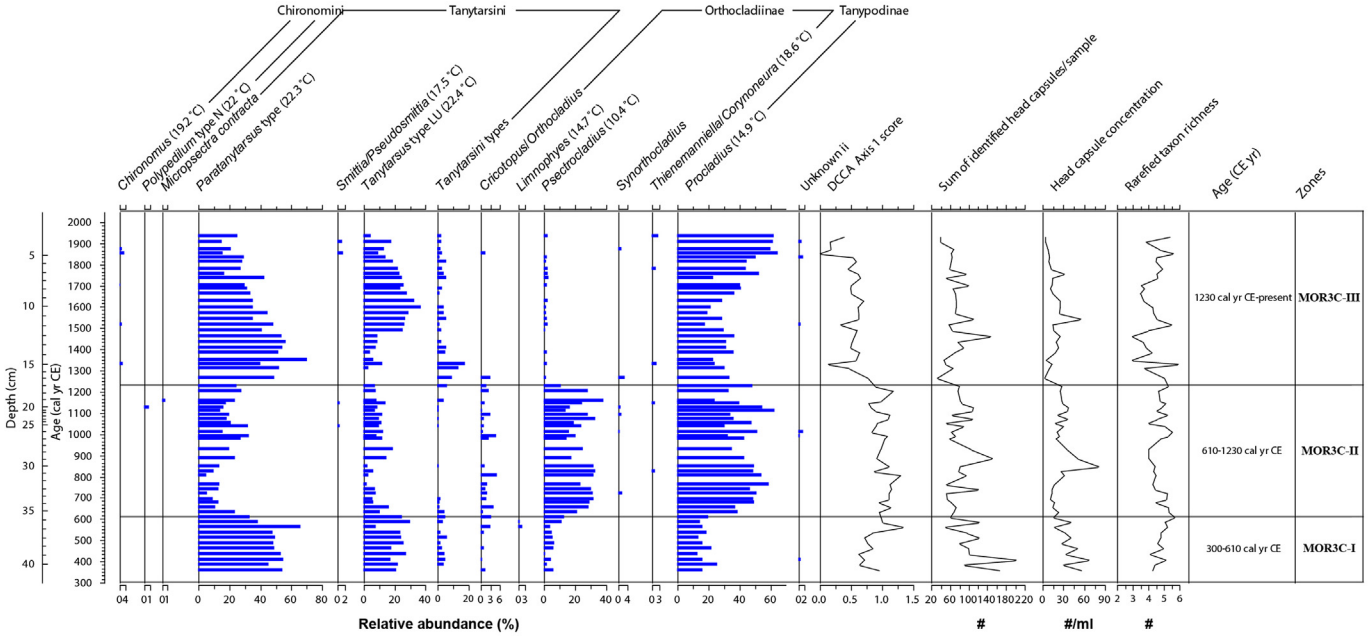

Fig. 3. Relative abundance of chironomids preserved in MOR3C for the interval from 300 CE to the present. Taxa names are organized by alphabetic order and the temperatures in the parentheses reflect their mean annual air temperature optima generated in Wu et al. (2015).

Notable turnover in the chironomid assemblages is detected at the onset of MOR3C-III (1230 CE-present; 16.25–0 cm). The relative abundance of *Psectrocladius* abruptly decreases at ~1230 CE, and *Paratanytarsus* shows a large increase, followed by an increase in *Tanytarsus* type LU at ~1400 CE. The relative abundance of *Psectrocladius* drops from ~25% in MOR3C-II to ~1% in MOR3C-III. *Paratanytarsus* and *Tanytarsus* type LU increase, comprising ~30% and 20% of the chironomid assemblage in MOR3C-III. The relative abundances of both taxa, however, begin decreasing after ~1600 CE. The amount of *Procladius*, which gradually decreases after the termination of MOR3C-II, begins to progressively increase from ~40% to 60% of the identifiable chironomid remains in the uppermost portion of the core. The increase in *Procladius* coincides with a decrease in *Paratanytarsus and Tanytarsus* type LU. *Chironomus* appears for the first time in this zone. *Smittia/Pseudosmittia*, *Cricotopus/Orthocladius*, *Thienemannella/Corynoneura*, *Synorthocladius,* and Unknown ii, present in MOR3C-II, remain present in MOR3C-III, although the relative abundance of *Cricotopus/Orthocladius* is greatly reduced. Head capsule concentration is lower than in MOR3C–I and MOR3C-II, with an average of 15.6 head capsules/ml and a maximum of 55 head capsules/ml, observed at ~1450 CE. The DCCA documents notable compositional turnover at ~1230 CE, with the remainder of MOR3C-III characterized by limited turnover. Rarefied taxon richness in MOR3C-III varies significantly, between 3.0 and 5.9, with the highest variability occurring between ~1250 and 1500 CE.

4. Discussion

4.1. Chironomid-based thermal reconstruction at Lago Morrenas 3C

The chironomid assemblage in MOR3C–I (300–610 CE) is dominated by three taxa, *Paratanytarsus*, *Tanytarsus* type LU, and *Procladius* (Fig. 3). The modern training set (Wu et al., 2015) does not provide a sufficient number of modern analogues to enable a quantitative reconstruction of MAAT, and as a result, we interpreted the chironomid paleoecology qualitatively. In Costa Rica, *Paratanytarsus* and *Tanytarsus* type LU are restricted to low- and mid-elevation lakes characterized by moderate to high MAAT and conductivity (Wu et al., 2015). The MAAT optima for *Paratanytarsus* and *Tanytarsus* type LU are 22.3 °C and 22.4 °C, respectively, which are amongst the highest MAAT optima of all the taxa in the training set (Wu et al., 2015). *Procladius* is considered an indicator of cold conditions, with a MAAT optimum of 14.9 °C (Wu et al., 2015). *Psectrocladius*, which is also associated with a very low MAAT optimum (10.4 °C; Wu et al., 2015), is present at low abundance in MOR3C–I. The dominance of thermophilous chironomid taxa in MOR3C–I suggests that the interval between ~300 and 610 CE was characterized by relatively high temperatures.

The notable increase in the relative abundance of *Psectrocladius* and *Procladius*, along with the concurrent decrease in *Paratanytarsus* and *Tanytarsus* type LU, starting at ~610 CE in MOR3C-II, is inferred to represent the onset of an interval of lower temperatures. Today, *Psectrocladius* and *Procladius* are most abundant in cold, high-elevation habitats, and largely restricted to the glacial lakes located in the Chirripó páramo (>3400 m a.s.l.), with an average MAAT of 7.7 °C (Wu et al., 2015). *Psectrocladius* inhabits the littoral zone and is often associated with aquatic macrophytes (Brooks et al., 2007). *Procladius* is very abundant (>60%) in the glacial lakes of different depths (0.3–22 m) that have been sampled in Chirripó NP (Wu et al., 2015). Six additional taxa associated with cold, high-elevation lakes and low MAAT in the Costa Rican modern training set, are also found in MOR3C-II (Wu et al., 2015): *Smittia/Pseudosmittia*, *Corynoneura/Thienemanniella*, Unknown ii, *Cricotopus/Orthocladius*, and *Synorthocladius*. *Cricotopus/Orthocladius* and *Synorthocladius* are most common in the littoral zone of lakes, with *Cricotopus/Orthocladius* favoring macrophytes (Cranston, 2010). *Smittia/Pseudosmittia* is primarily associated with terrestrial/semi-terrestrial habitats (Spies et al., 2009) and Unknown ii is only found in relatively shallow lakes (<3 m) (Wu et al., 2015). The high relative abundance and diversity of cold-indicator chironomid taxa, together with the notable decrease in thermophilous taxa, is inferred to reflect depressed MAAT between ~610 and 1230 CE (MOR3C-II). The presence of taxa associated with shallow lakes, the littoral zone, and macrophytes, including terrestrial/semi-terrestrial taxa, implies the occurrence of lower lake levels, with a possible expansion of aquatic macrophytes during this interval. Taken together, MOR3C-II appears to represent a cold and relatively dry interval, with the maximum lake level decline occurring between ~700 and 1100 CE.

The recovery in the relative abundance of the thermophilous taxa *Paratanytarsus* and *Tanytarsus* type LU, and the decrease in the cold-indicator taxa *Procladius* and *Psectrocladius*, are inferred to reflect the onset of relatively warmer conditions beginning at ~1230 CE and peaking between 1520 and 1630 CE. The increase in *Procladius* beginning at ~1600 CE marks a gradual shift to cooler conditions. The decrease and/or absence of many of the littoral and terrestrial/semi-terrestrial chironomid taxa between 1230 and ~1850 CE, including *Psectrocladius*, which decreases abruptly at ~1230 CE, suggests that effective moisture increased at Lago Morrenas 3C during this interval, resulting in higher lake level, greater water volume, and decreased littoral habitat.

4.2. Late Holocene hydroclimate variability across an elevation gradient in Costa Rica

Patterns of climate and environmental change over the past two millennia at Lago Morrenas 3C resemble some aspects of the record from Laguna Zoncho (Fig. 1AD), a mid-elevation lake located near the southern border of Costa Rica (Fig. 4AB). The chironomid assemblage in MOR3C indicates that the interval between 300 and 610 CE is characterized by relatively high temperature. The chironomid-inferred MAAT at Laguna Zoncho between 50 BCE and 610 CE is 0.4 °C above the late Holocene average (21.3 °C) (Fig. 4B; Wu et al., 2017). Thus, both sites experienced relatively warm conditions during this interval. Hydrological and fire regimes, however, differ at the two sites, in part because of their differing histories of human occupation. Lago Morrenas 3C, a remote lake in an area never settled by humans, is characterized by moderate $\delta^{13}C$ values, extremely low charcoal influx and no large fire events (Fig. 4A; Wu and Porinchu, 2007). During this same interval, Laguna Zoncho was characterized by a low abundance of a benthic diatom endemic to Laguna Zoncho, *Aulacoseira sp.* 3, implying the existence of a relatively shallow, possibly turbid aquatic environment (Haberyan and Horn, 2005), and gradually increasing $\delta^{13}C$ values, reflecting the expansion of maize (*Zea mays* subsp. *mays*) along with other C_4 grasses and herbs associated with prehistoric agriculture in the watershed (Clement and Horn, 2001; Lane et al., 2004). The increasing $\delta^{13}C$ values could also in part signal a shift toward drier conditions, which can also favor C_4 herbs and can shift the fractionation of C_3 plants toward more positive $\delta^{13}C$ values (Diefendorf et al., 2010; Kohn, 2010). The elevated charcoal amount observed during this time at Laguna Zoncho is likely related to anthropogenic activities, perhaps both forest clearance and the maintenance of agricultural fields.

Notable and similar changes in climate and environmental conditions are evident at both Lago Morrenas 3C and Laguna Zoncho between 610 and 1230 CE (Fig. 4; Wu et al., 2017). In the Morrenas 3C catchment, increased $\delta^{13}C$ values observed between 700 and 1100 CE are interpreted to indicate the expansion of the C_4

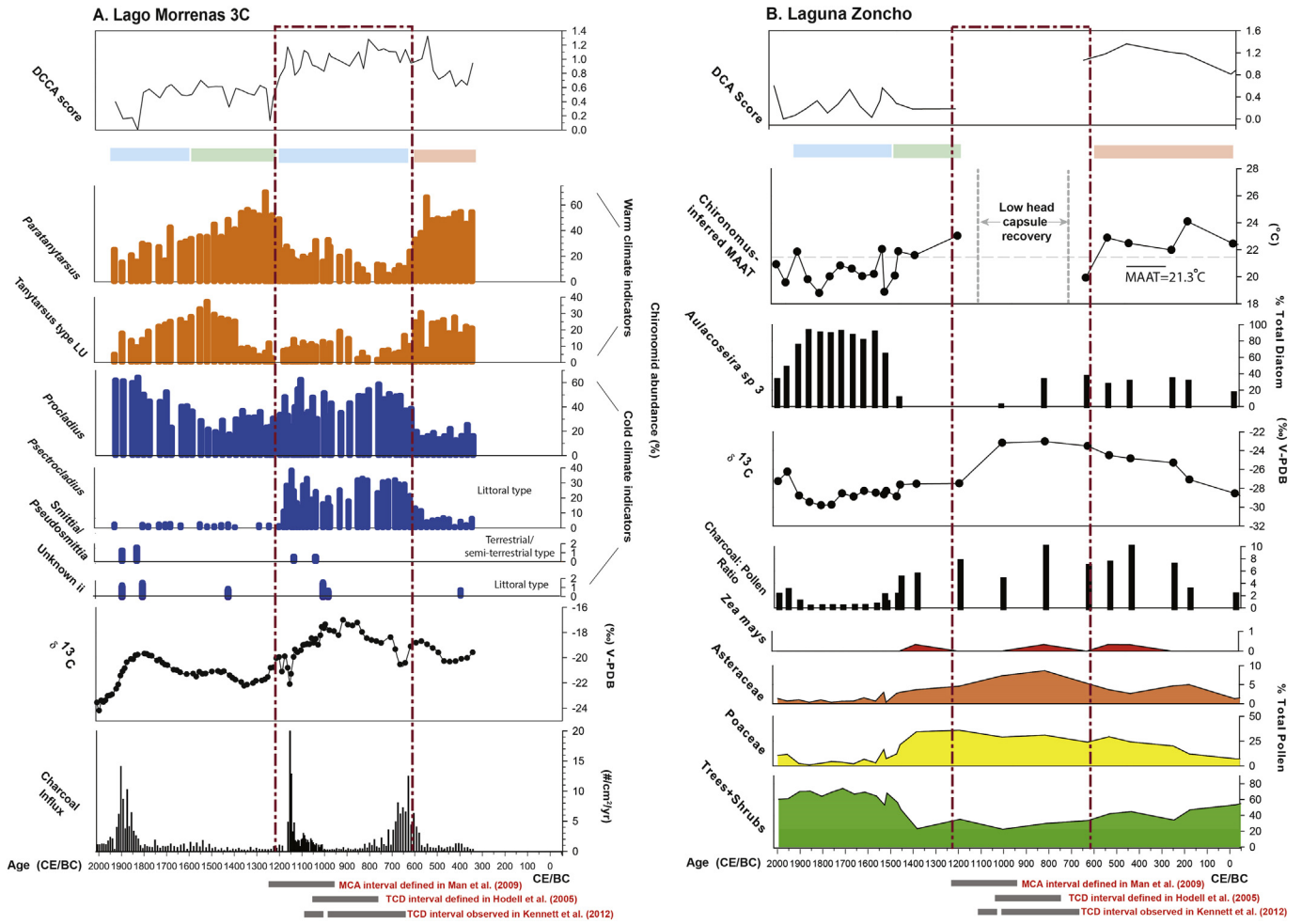

Fig. 4. Select proxy data from **(A)** Lago Morrenas 3C and **(B)** Laguna Zoncho (Wu et al., 2017). The red box frames the interval between 610 and 1230 CE (MOR3C-II). Grey horizontal bars below the X-axes represent the MCA (950–1250 CE; Mann et al., 2009), TCD (770–1100 CE; Hodell et al., 2005) and extended TCD (660–1000 CE, 1020–1100 CE; Kennett et al., 2012) intervals. Horizontal bars colored by orange, green and blue bars represent intervals that are characterized by relatively warm, intermediate, and cool conditions, respectively. Charcoal influx of MOR3C = total number (#) of >125 μm charcoal particles/sediment sample volume (cm^3) × sedimentation rate (cm/yr). (For interpretation of the references to color in this figure legend, the reader is referred to the Web version of this article)

grass *Muhlenbergia*, in response to cool, dry conditions at the time. As mentioned, greater $\delta^{13}C$ values can also reflect the response of C_3 plants to drier conditions (Diefendorf et al., 2010; Kohn, 2010). The relatively high abundance of the semi-terrestrial/terrestrial taxa *Smittia/Pseudosmittia* and Unknown ii, suggests that lake level decline was greatest at ~1000 CE at Lago Morrenas 3C. Severe fires inferred from charcoal influx documented at ~650 CE and 1150 CE, which broadly bracket the TCD-MCA interval, also occur during this cool, dry period (Wu and Porinchu, under review). The timing of the shift in the chironomid assemblage corresponds to the presence of high concetrations of algae/fecal pellets in the core, a possible signal of lower lake levels (M. Bush, personal communication). The presence of high amounts of algal/fecal pellets throughout MOR3C-II, suggests the existence of a shallow lake and likely, drier conditions. At Laguna Zoncho, the chironomid-inferred thermal reconstruction (Wu et al., 2017) indicates that MAAT decreased by ~1.9 °C relative to the late Holocene average between ~550 CE and ~650 CE. We lack quantitative chironomid-based estimates of MAAT at Laguna Zoncho for the interval from 730 to 1100 CE (denoted by faint grey lines within a red box in Fig. 4B) because of the near absence of chironomid head capsules during this interval. This lack of sub-fossil chironomid remains, together with the limited abundance of *Aulacoseira sp.* 3 and other aspects of the diatom assemblage (Haberyan and Horn, 2005), suggest notably lower lake level and a greatly reduced pool of standing water from 730 to 1110 CE, reflecting reduced effective moisture (Wu et al., 2017).

Over the past ~720 years, similar patterns of climate and environmental change are observed at both Lago Morrenas 3C and Laguna Zoncho (Fig. 4AB). The chironomid stratigraphy from MOR3C-III suggests that the climate was characterized by temperate to warm conditions between 1230 and ~1630 CE, based on the reduced abundance of *Procladius* and *Psectrocladius*, cold climate indicators, and elevated amounts of *Paratanytarsus* and *Tanytarsus* type LU, warm climate indicators. The absence or relatively low abundance of littoral and terrestrial/semi-terrestrial chironomids between 1230 and ~1850 CE likely reflect the influence of increasing effective moisture and lake level. The near absence of wildfires during this ~600-yr period supports the chironomid-based inference of wetter conditions, i.e. fuel was too wet to burn. At Laguna Zoncho, chironomid-inferred MAAT indicates an interval of moderate MAAT between ~1200 and 1550 CE, followed by an extended interval of below average MAAT beginning at ~1550 CE. The increase in the benthic diatom *Aulacoseira sp.* 3, which begins at 1550 CE, and other changes in diatom percentages, likely reflect the onset of an interval characterized by higher lake level, driven by increased effective moisture (Haberyan and Horn,

2005; Wu et al., 2017). The increased abundance of tree and shrub pollen and reduced charcoal after ~1550 CE appears to largely reflect population decline and forest regeneration following the Spanish Conquest, but could also reflect a shift toward higher effective moisture. The drop in MAAT that is inferred at Laguna Zoncho and Morrenas 3C between ~1600 CE and the present provides evidence of the manifestation of the Little Ice Age (LIA) in southern Central America. During the LIA interval, effective moisture likely dropped at Lago Morrenas 3C, inferred from relatively high abundance of terrestrial/semiterrestrial and littoral chironomid taxa, more positive $\delta^{13}C$ values, and higher charcoal influx. However, effective moisture may have increased at Laguna Zoncho, reflected in the abundance of tree/shrub pollen and *Aulacoseira sp. 3* (benthic diatom type; Haberyan and Horn, 2005).

The basin characteristics and geographic locations of these two lakes may explain their sensitivity to climate and environmental change during the late Holocene. Laguna Zoncho and Lago Morrenas 3C are both small (area <1 ha), shallow lakes (depth <3 m; Table 1; Fig. 1). There is a strong correspondence in thermal conditions in the mid- and high-elevation regions of Costa Rica for the period between ~300 and 610 CE, which was characterized by relatively high temperatures; for the period between ~1230 and 1600 CE, which was characterized by moderate temperatures; and for the interval after ~1600 CE, which was characterized by the onset of cooling (horizontal color bands in Fig. 4AB). In addition, the multi-proxy paleoclimate records developed for both lakes generate a relatively consistent picture of hydroclimate variability during the TCD and the early portion of the MCA. The composition of the chironomid community and the $\delta^{13}C$ values provide evidence for a reduction in effective moisture and low lake level between ~700 and 1100 CE at Lago Morrenas 3C, which corresponds to the timing of lake level decline at Laguna Zoncho (Wu et al., 2017). The reduction in effective moisture that characterized the interval spanned by the TCD and the MCA at Laguna Zoncho appears to be more severe than the hydroclimate change observed at Lago Morrenas 3C. Although the dry season at Laguna Zoncho (Taylor et al., 2013a) appears to be equally pronounced at Cerro missing accent (Esquivel- Hernández et al., 2018) in terms of precipitation amount and duration of the dry season, elevated evaporation resulting from higher MAAT at lower elevation along the Pacific slope may account for the lake level decline observed at Laguna Zoncho during the TCD-MCA interval. Additionally, the intermittent presence of relatively high cloud cover during the dry season at Lago Morrenas 3C, depending on the height of the northeast trade wind inversion and other atmospheric conditions, could have reduced the evaporation rate at the site by depressing the average monthly maximum temperature (Coen, 1983).

4.3. Hydroclimate change in the northern tropical Americas during Medieval times

Many proxy-based reconstructions of late Holocene hydroclimate show evidence of environmental changes driven by climate fluctuations during Medieval times, generally between ~500 and 1500 CE in the northern tropical Americas (Curtis et al., 1996; Haug et al., 2003; Lachniet et al., 2004; Hodell et al., 2005; Lane et al., 2011a; Kennett et al., 2012; Douglas et al., 2016; see Table 3 for more details). Earlier research, focusing on reconstructing vegetation dynamics and the fire history of the páramo in Chirripó NP from the sediments of Lago Chirripó and Lago Morrenas 1, documented fires throughout the Holocene and the occurrence of severe drought, lower lake levels, and increased wildfires at ~850 CE and 550 BCE (Horn and Sanford, 1992; Horn, 1993; League and Horn, 2000). The more recent interval corresponds to the time of the most positive $\delta^{13}C$ values in the MOR3C core, which is inferred to reflect an expansion of the C_4 grass *Muhlenbergia flabellata*, under cooler and drier conditions. Studies of $\delta^{13}C_{C27-C33}$ and δD_{25-33} of *n*-alkanes from Lago Morrenas 1, however, suggested that the Valle de las Morrenas was characterized by mesic conditions between ~550 and 1150 CE (Lane et al., 2011a; Lane and Horn, 2013). Between ~1090 and 1310 CE, Taylor et al. (2013a) also identified a notable decline in agricultural activities in southern Costa Rica, predating the arrival of the Spanish by approximately 200 years, which is inferred to reflect the influence of regional drought on agriculture.

Bhattacharya et al. (2017) synthesized the results of published paleoenvironmental studies and provided robust evidence for severe drying in Mesoamerica between ~800 and 1200 CE. The sites included are mainly located northern Nicaragua, Mexico (i.e., the cultural region of Mesoamerica) and in the Caribbean and tropical Atlantic, with the sites experiencing severe droughts clustered in northern Central America and Mexico. Most of those studies, which used speleothems, lake, and marine sediments, and climate proxies including stable isotopes, sediment geochemistry, biomarkers, and flora and faunal remains, focused on exploring the relationship between hydroclimate variability and cultural phases of the Maya civilization during the TCD and MCA. Additional sites with detailed paleoclimate and paleoenvironmental records from southern Central America and elsewhere in tropical America are identified in Table 3.

A synthesis of the spatio-temporal pattern of hydroclimate variability for the interval between 500 and 1500 CE, incorporating the sites in Table 3, is presented in Fig. 5. Notable drought occurs between 500 and 1300 CE in central and southern Mexico, Belize, Guatemala, Nicaragua, Costa Rica, Panama and the western Dominican Republic. The precise timing of drought and environmental change that occurred at the turn of the last millennium is temporally variable in the tropical Americas. Yet, most of the study sites in the northern tropical Americas experienced a drought interval centered between ~750 and 1200 CE (Fig. 5B). The dry interval identified in Costa Rica between 700 and 1100 CE coincides well with dry conditions at Punta Laguna in Mexico (Curtis et al., 1996), Lake Chichancanab in Mexico (Hodell et al., 2005), and Yok Balum Cave in Belize (Kennett et al., 2012), and overlaps with dry conditions between 430 and ca. 1000 CE in the western Dominican Republic (Lane et al., 2009, 2011b). Hydroclimate conditions during this interval are, however, spatially heterogeneous within the broader region, with western Cuba (Fensterer et al., 2012), Barbados (Ouellette, 2013), Venezuela (Haug et al., 2003) and Panama (Lachniet et al., 2004) characterized by wetter conditions, or alternating wet/dry cycles (Venezuela, Haug et al., 2003; Panama, Lachniet et al., 2004). In addition to the observed changes in hydroclimate, notable changes in SSTs and terrestrial MAATs are also documented during this interval. A decrease in SSTs is observed in the western and southeastern Caribbean from 900 to 1200 CE (Site 12 in Fig. 5; Sorey, 2014) and from 800 to 1200 CE (Site 22 in Fig. 5; Tedesco and Thunell, 2003.

4.4. Drivers of hydroclimate change in Costa Rica during the TCD and MCA

The TCD-MCA interval (~770–1250 CE) was characterized by a spatially heterogeneous expression of hydroclimate change, although it is generally associated with warmer conditions in the mid-to-high latitudes in the Northern Hemisphere (Hughes and Diaz, 1994; Mann et al., 2008). Fluctuations in global climate at ~1000 CE are believed to reflect the influence of enhanced solar activity and reduced volcanic activity (Mann et al., 2005, 2009; Haltia-Hovi et al., 2007; Cook et al., 2010). The forcing of regional climate during the TCD-MCA interval is still not fully understood, with the cause(s) of the observed hydroclimate anomalies in the

Table 3
Paleoenvironmental reconstructions of hydroclimate variability during TCD/MCA phase in the tropical Americas. Sites are numbered according to latitude with sites correspondingly numbered in Fig. 5.

Site No.	Site Location	Proxy	TCD/MCA expression 500–1200 CE	Sources
1	Dos Anas Cave, northwestern Cuba	$\delta^{18}O$ in stalagmite	Wetter condition between 950 and 1050 CE is observed, and lower SSTs in the North Atlantic possibly lead to a southward shift of ITCZ	Fensterer et al. (2012)
2	Punta Laguna, Mexico	$\delta^{18}O$ of the ostracod and gastropod shells in lake sediments	Relatively dry climate was found from ~280 to 1080 CE Multiple significant dry events identified at ~600 CE, 860 CE	Curtis et al. (1996)
3	Tecoh cave, northwest Yucatán Peninsula	$\delta^{18}O$ in stalagmite	Rainfall greatly reduced, eight severe droughts occurred btw 800–950 CE with an even servere one 640–680 CE	Medina-Elizalde et al. (2010)
4	Lake Chinchancanab, Mexico	Bulk density, red and blue color reflection in lake sediments	A series of dry events concentred in periods of 770–870 CE, and 920–1100 CE	Hodell et al. (2005)
5	The Sierra de Manantlan Biosphere Reserve, west-central Mexico	Pollen	Dry interval observed between 750 and 1100 CE	Figueroa-Rangel et al. (2008)
6	Lake Aljojuca in Central Mexico	Elemental geochemistry and $\delta^{18}O$ from authigenic calcite	A lont-term drought observed from 500 to 1150 CE may have caused abandonment of Cantona and population collapse in Cantona	Bhattacharya et al. (2015)
7	Laguna Castilla, Dominican Republic	Long-chain ($\geq C_{25}$) n-alkane δD, $\delta^{18}O$ in ostracods, pollen, mineral influx in lake sediments	Increased aridity found during TCD (~750–1100 CE)	Lane et al. (2009, 2014)
8	Laguna Felipe, Dominican Republic	$\delta^{18}O$ in ostracods and $\delta^{13}C$ in lacustrine biogenic carbonates	Wetter MCA detected from 1000 to 1300 CE based on absence of carbonate material and mineral-rich clay indicates a northward migration of ITCZ	Lane et al. (2011b)
9	Lake Salpeten, Guatemala Lake Chinchancanab, Mexico	Plant wax carbon isotopes in lake sediments	Aridrity between ~800 and 1200 CE forced extensive agriculture to shift to intensive, waterconservative maize cultivation	Douglas et al. (2015)
10	Belize Central Shelf Lagoon	Particle size and elements (e.g.Ti, K, Ti/Al) in lacustrine (lagoon and channel) sediments	Unusually low Ti counts and Ti/Al inferred low precipitation btw 800 and 900 CE. High Ti, Ti/Al between 900 and 1350 CE inferred more rainfall and wet condition	Agar Cetin (2014)
11	Lake Salpetén, Guatemala	$\delta^{18}O$ on valves of the ostracod, Inorganic carbon in lake sediments	Severe aridity identified between 800 and 900 CE	Rosenmeier et al. (2002)
12	Blue hole, western Caribbean Sea near Belize	$\delta^{15}N$ in marine sediments	Intensified upwelling btw 900 and 1200 CE, corresponded strengthening trade wind (Positive NAO)	Sorey (2014)
13	Laguna Yaloch (Holmul region), Guatemala	Magnetic susceptibility, $\delta^{13}C$, C %, N%, pollen, charcoal	Evidence for anomalously dry conditions found from ~680 to 910 CE	Wahl et al. (2013)
14	Macal Chasm Cave, Belize	reflectance, color, luminescence, and $\delta^{13}C$ and $\delta^{18}O$ in stalagmites	A series of droughts concentrated from 700 to 1135 CE	Webster et al. (2007)
15	Juxtlahuaca Cave, Mexico	$\delta^{18}O$ in JX-6 stalagmites	Dry condition peaked during period of 600–900 CE and megadrought observed at 770 CE	Lachniet et al. (2012)
16	Juxtlahuaca Cave, Mexico	$\delta^{18}O$ in JX-6 and JX-7 stalagmites	Intense dry condition observed from 700 to 850 CE, Five short-lived dry events during period of 930–1300 CE	Lachniet et al. (2017)
17	Yok Balum Cave, southern Belize	$\delta^{13}C$ in stalagmites	Notably dry from 850 to 950 CE and 1000 to 1150 CE but with negative NAO observed (short-lived climate shifts related to NH volcanic eruptions)	Ridley (2014)
18	Yok Balum Cave, southern Belize	$\delta^{18}O$ in stalagmite	Drying trend between 660 and 1000 CE triggered collapse of	Kennet et al. (2012)

Table 3 (*continued*)

			polities, followed by population collapse during an extended drought between 1020 and 1100 CE.	
19	Harrison's Cave, Barbados	$\delta^{18}O$ in speleothem	Wet condition observed between 850 and 1150 CE	Ouellette thesis (2013)
20	Lago El Gancho, Nicaragua	$\delta^{18}O$ in ostracods	Wetter condition between 950 and 1250 CE inferred from low $\delta^{18}O$, indicating a La Nina-like condition in the tropical Pacific	Stansell et al. (2013)
21	Cariaco Basin, Venezuela	Ti% in marine core sediments	An extended regional dry period is found with more punctuated intense multi-year droughts at approximately 810, 860, and 910 CE	Haug et al. (2003)
22	Cariaco Basin, Venezuela	$\delta^{18}O$ in ostracods	Strong upwelling caused SST cooling observed between 800 and 1200 yr BP	Tedesco and Thundell (2003)
23	Lago Morrenas 1 core 2, Costa RicaLago Chirripo, Costa Rica	Microscopic charcoal and pollen	Charcoal peak identified at 1100 CE and abundant isoetes pollen at approximately 900 CE, suggesting dry condition	Horn (1993); Horn and Sanford (1992)
24	Lago Morrenas 1 core 1, Costa Rica	δD of long-chain alkane in bulk sediment	Low dD inferred reduce in E/P ratio arround 1000 CE, suggesting wetter climate	Lane and Horn (2013)
25	Lago Morrenas 1 core 1, Costa Rica	$\delta^{13}C$ of long-chain alkane in bulk sediment	C_4 plants may lightly shrink approximately between from 800 to 1200 CE, indicating wetter condition	Lane et al. (2011a)
26	Lago Morrenas 3C and Lago Ditkebi, Costa Rica	Charcoal and geochemical (C%, N%, $\delta^{13}C$, $\delta^{15}C$)	Low lake level observed from ~750 to 1100 CE, intense drought may occur between 850 and 1100 CE, severe local fires found during periods of 550–750 CE and 1050–1200 CE	Wu and Porinchu, *under review*
27	Lago Morrenas 3C	Subfossil chironomids	Cold phase detected from ~610 to 1230 CE	This study
28	Chilibrillo Cave, Canal Zone, Panama	$\delta^{18}O$ in stalagmite	Weakenend monsoon observed from 1100 to 1200 CE, andfrom 750 to 950 CE, with even drier period during 550–650 CE	Lachniet et al. (2004)
29	Laguna Zoncho, Costa Rica	Chironomids-based temperature inference model	Extremely low head capsules recovery between 730 and 1110 CE,like indicating low effective moisture in the lake	Wu et al. (2017)

northern tropical Americas between ~500 and 1500 CE a source of debate (Jones et al., 1999; Gosse et al., 2004; Diaz et al., 2011). The general trends highlighted in global-scale syntheses (Mann et al., 2009) often mask the heterogeneous response of the climate system at finer spatial scales (Giorgi and Avissar, 1997), and consequently, global studies may be insufficient for documenting the response of the climate system to various forcings at regional scales. Improving our understanding of regional climate dynamics, as well as recognizing the importance of spatial variability of hydroclimate change in controlling regional patterns, will significantly improve our ability to model regional response to future climate forcings (Cubasch et al., 2001; Giorgi et al., 2001; Radić et al., 2014). Comparison of the late Holocene proxy records of hydroclimate change from Costa Rica developed in this study, to existing records, provides the opportunity to assess the various mechanisms that have been invoked to account for climate and environmental change in Mesoamerica between ~500 and 1500 CE.

Enfield and Alfaro (1999) and Giannini et al. (2000) proposed a link between variations in the strength of Atlantic Meridional Overturning Circulation (AMOC) and hydroclimate variability in Central America and the Caribbean. A decrease in the density of North Atlantic surface waters, in response to increased ice-rafting debris, such as during Bond events (Fig. 6f), would reduce the strength of AMOC because of increased freshwater input at the loci of North Atlantic Deep Water (NADW) formation (Bond et al., 1997; Bianchi and McCave, 1999; Keigwin and Boyle, 2000). A reduction in the strength of AMOC would result in reduced northward transport of warm tropical water in the Atlantic, facilitate the development of an anomalously warm pool in the Caribbean, and change the sea temperature gradient in the Atlantic (Bond et al., 1997, 2001; Bianchi and McCave, 1999; Keigwin and Boyle, 2000). The consequent increase in the SST gradient would result in the mean summer position of the ITCZ migrating southward, resulting in drought in the northern tropical Americas and Caribbean (Enfield and Alfaro, 1999; Giannini et al., 2000). Important ice drifting events in the North Atlantic, however, appear to have limited overlap with the dry interval (~700–1100 CE) identified in Costa Rica and elsewhere in the northern tropical Americas, and occurred during an interval of anomalously low SSTs in the Caribbean (Table 3 and Fig. 5; site 22: Tedesco and Thunell, 2003; site 12: Sorey, 2014). This suggests that ice rafting episodes were not directly responsible for the extended droughts observed in the northern tropical Americas between ~700 and 1100 CE.

The existence of an inter-oceanic temperature gradient between

the eastern tropical Pacific and the tropical Atlantic has also been invoked to explain the observed hydroclimate variability between ~600 and 1200 CE in the northern tropical Americas (Enfield and Alfaro, 1999; Giannini et al., 2000; Taylor et al., 2002; Wahl et al., 2014). Meteorological data indicate that summer precipitation in the Caribbean and Central America decreases when the tropical Atlantic is anomalously cool and the eastern tropical Pacific is anomalously warm (Enfield and Alfaro, 1999; Giannini et al., 2000). Douglas et al. (2015, 2016) and Lachniet et al. (2017) hypothesized that an SST gradient between the Atlantic and the Pacific basins,

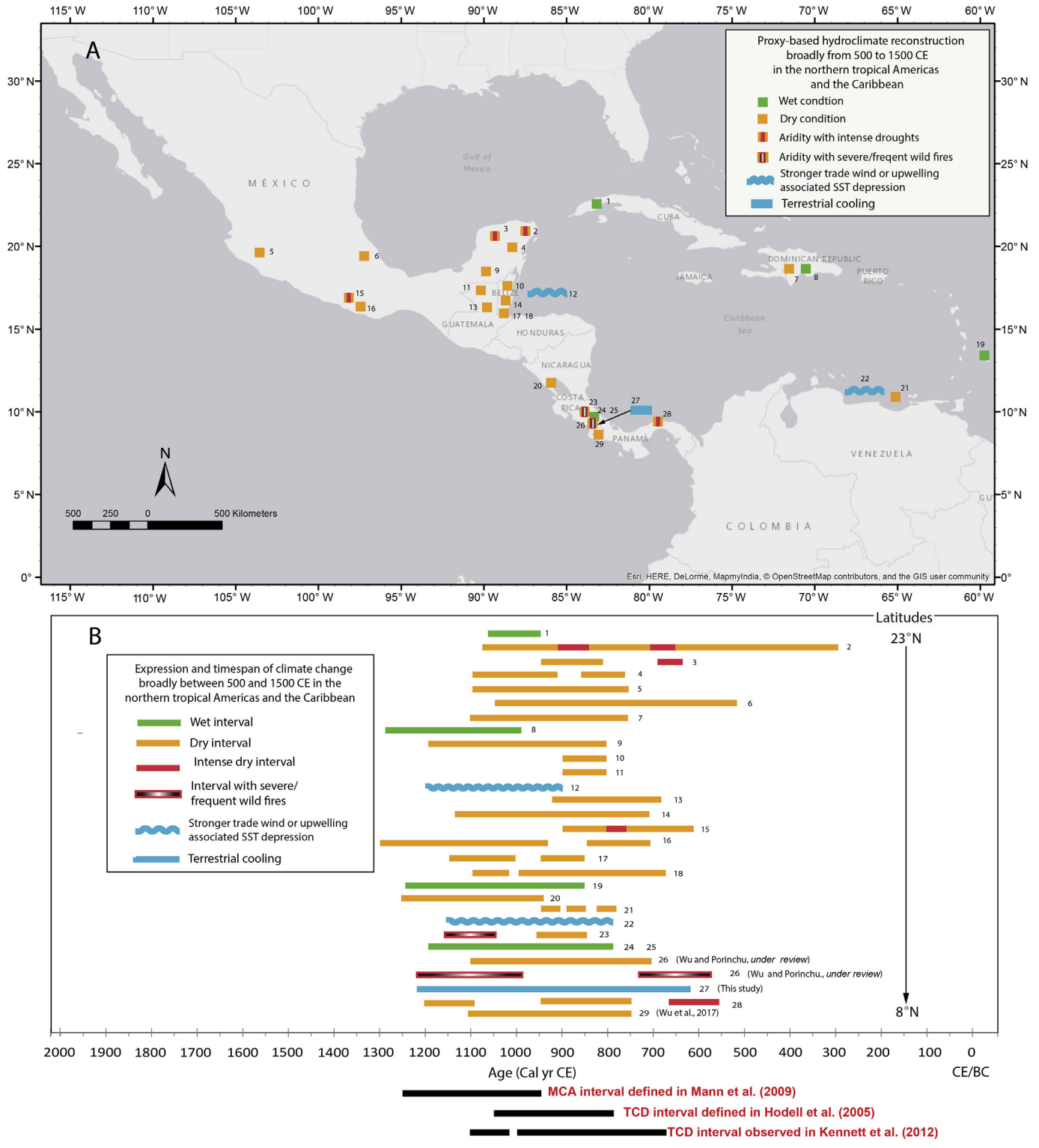

Fig. 5. A) Location of studies characterizing hydroclimate variability and paleoenvironmental conditions in the northern tropical Americas and Caribbean between ~500 and 1500 CE; the duration of the hydroclimate anomaly is indicated by the length of the bar, shown in. B) The study sites are numbered according to latitude, with northernmost site numbered 1. The site numbers in Fig. 5A and B correspond to the references in Table 3.

associated with El Niño-like conditions, could result in the hydroclimate anomalies observed in Mesoamerica during the TCD and MCA. Proxy-based reconstructions of late Holocene ENSO activity in the Galapagos Islands (Fig. 6g; Conroy et al., 2008) and Ecuador (Fig. 6h; Moy et al., 2002), however, do not provide support for more frequent El Niño events (warm anomalies) in the eastern tropical Pacific during the TCD-MCA interval. In addition, climate model simulations using paleoclimate proxy data suggest the existence of La Niña-like conditions characterized by depressed SSTs in the eastern tropical Pacific between ~950 and 1250 CE (Seager et al., 2007; Mann et al., 2008, 2009). At present, the limited number of high-resolution SST reconstructions for the eastern tropical Pacific precludes a thorough test of the hypothesis that droughts between ~600 and 1200 CE in Mesoamerica were driven by a temperature gradient between the eastern tropical Pacific and the tropical North Atlantic.

Recently, Bhattacharya et al. (2017) identified a mechanism that can account for the spatio-temporal pattern of widespread drought observed in the northern tropical Americas and anomalous cooling in the tropical North Atlantic between ~600 and 1200 CE. Bhattacharya et al. (2017) identified two intervals characterized by a statistically significant probability of widespread drought in the northern tropical Americas: 400–600 CE and 800–1200 CE. General circulation model (GCM) simulations highlight the influence of SSTs in the tropical North Atlantic on the spatial pattern of hydroclimate variability in the northern tropical Americas during these two intervals. Anomalously low SSTs in the tropical North Atlantic lead to decreased evaporation and reduced boundary layer moisture over the Caribbean, with stronger northeast trade winds further contributing to cooling as a result of positive wind-evaporation-SST feedback (Xie and Carton, 2004). Stronger northeast winds, together with reduced boundary layer moisture, would facilitate elevated moisture divergence, with moisture transport increasing towards the northern Gulf of Mexico, but decreasing in

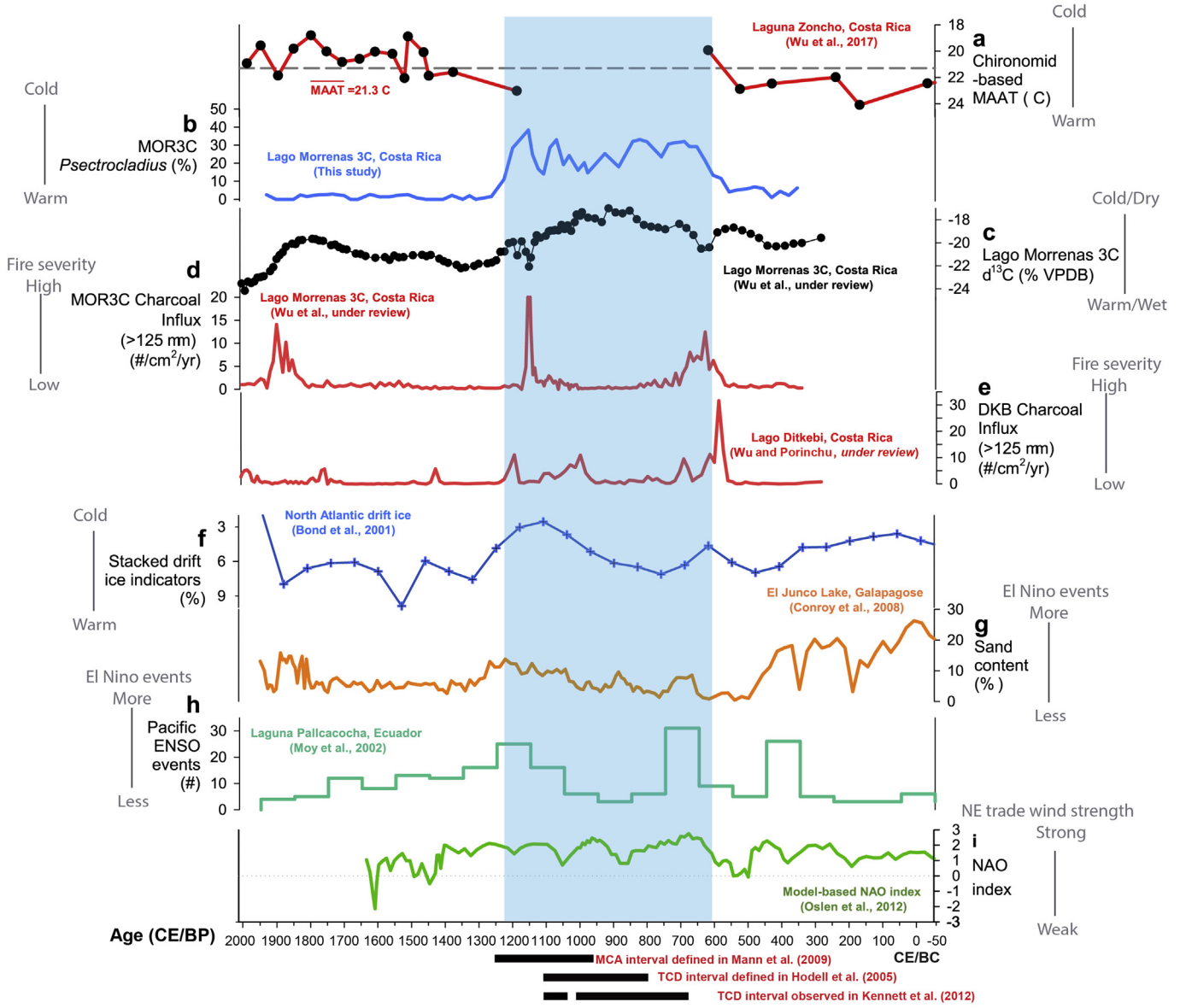

Fig. 6. Synthesis of the proxy records developed in this study and selected proxy records from sites in the tropical Americas and the North Atlantic. The black horizontal bar at the bottom of the figure represents the MCA and TCD, as defined and observed in Mann et al. (2009), Hodell et al. (2005) and Kennett et al. (2012). The MOR3C-II zone (610–1230 CE) identified in the MOR3C core is highlighted using a vertical blue bar. (For interpretation of the references to color in this figure legend, the reader is referred to the Web version of this article.)

the circum-Caribbean. The effect of depressed SSTs in the tropical North Atlantic on the North Atlantic Subtropical High (NASH), northeast trade wind strength, and boundary layer moisture transport coupled with a wind-evaporation-SST feedback, leads to a distinct dipole pattern with northern Mexico getting wetter and southern central America getting drier between 600 and 1200 CE (Bhattacharya et al., 2017).

Analysis of the instrumental record identifies the existence of a dipole pattern in precipitation in this region associated with the negative phase of the Atlantic Multidecadal Oscillation (AMO) and the positive phase of the North Atlantic Oscillation (NAO) (Fig. 7; Bhattacharya et al., 2017). The negative phase of the AMO, defined by negative SST anomalies (SST cooling) in the tropical North Atlantic and intra-America seas, reduces evaporation, decreases boundary layer moisture, and suppresses convection and tropical storm formation over southern Central America and northern South America (Mestas-Nuñez et al., 2007). The positive phase of NAO, which is characterized by an enhanced sea-level pressure (SLP) gradient between the Icelandic Low and the North Atlantic Subtropical High (NASH), results in a stronger NASH and northeast trade winds, lower SSTs, and reduced atmospheric humidity over the intra-America seas and southern Central America, leading to drying in this region (Giannini et al., 2000; Hurrell and Deser, 2010). The suggestion that the interval between ~600 and 1200 CE was characterized by a positive NAO is supported by a study documenting that NAO values were highly positive, ranging from 1 to 2.5, between 600 and 840 CE and between 900 and 1050 CE (Fig. 6i; Olsen et al., 2012). This hypothesis is also supported by model simulations that suggest lower SSTs, stronger NASH, and stronger northeast trade winds and reduced boundary layer moisture transport can account for the dry conditions observed in southern Central America during the last two millennia (Bhattacharya et al., 2017).

Another mechanism proposed to explain the severe droughts generally between 500 and 1500 CE in the northern tropical Americas relates to the southern migration of the ITCZ (Haug et al., 2003; Hodell et al., 2005, 2007). Today, a more southerly (northerly) mean position of the ITCZ is typically associated with drier (wetter) conditions in southern Central America (Coen, 1983; Martinson, 1993; Clawson, 1997; Lane et al., 2011a). The mean position of the ITCZ is tightly linked to the inter-hemispheric gradient of SSTs (Wagner et al., 1996; Xie and Carton, 2004; Broccoli et al., 2006; Chiang and Friedman, 2012; Schneider et al., 2014). Anomalous cooling of the Northern Hemisphere, including the tropical North Atlantic, results in a southward migration of the mean position of the ITCZ, which in turn results in reduced rainfall and enhanced drought in the northern tropics (Fig. 7; Xie and Carton, 2004; Chiang and Friedman, 2012; Schneider et al., 2014; Bhattacharya et al., 2017). A positive feedback may occur with the southward migration of the ITCZ leading to strengthened northeast trade winds and decreased cloud cover in the tropical Northern Hemisphere, allowing more long-wave radiation to escape to the atmosphere, further contributing to a decrease in SSTs in the tropical North Atlantic (Fig. 7; Xie and Carton, 2004). In fact, evidence of negative SST anomalies is documented in marine sediment cores from the Cariaco Basin between 750 and 1150 CE (Site 22 in Fig. 5; Tedesco and Thunell, 2003) and from the northwest Caribbean between 900 and 1200 CE (site 12 in Fig. 5; Sorey, 2014), generally corresponding to the timing of depressed MAAT at MOR3C. Therefore, in addition to the influence of the tropical SSTs in North Atlantic, a southward shift in the mean position of the ITCZ may have also played an important role in enhancing the drought that characterized the TCD-MCA interval in Central America (e.g. Haug et al., 2003; Hodell et al., 2005; Lane et al., 2014).

The chironomid-inferred cooling observed at Lago Morrenas 3C between 610 and 1230 CE may reflect the influence of the tropical North Atlantic and Pacific on terrestrial climate in southern Central America during this interval. Pounds et al. (2006) showed that variations in tropical SSTs and adjacent terrestrial air temperature between 30 °S and 30 °N are positively correlated based on instrumental data (1950–2000 CE). A model-based study determined that anomalies in land surface (air) temperature (LST) in southern Central America, including Costa Rica, match in sign with SST anomalies in the surrounding ocean (Los et al., 2001). Additional support for coupling of land surface temperature (LST) in southern Central America and SSTs in the tropical Atlantic can be found in work by Smith et al. (2008). A simulation of low-frequency and inter-decadal-scale anomalies of global temperature, including

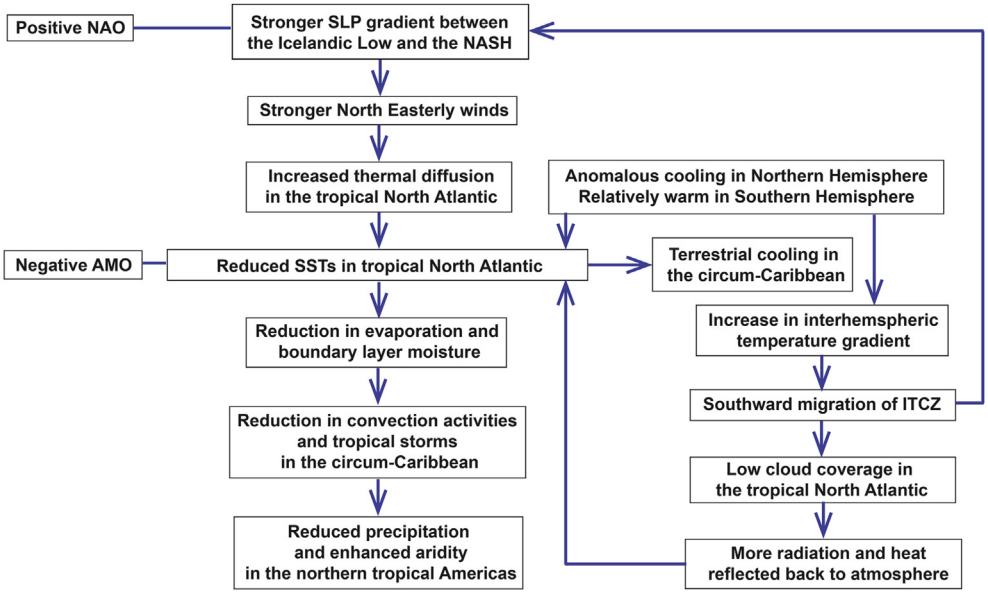

Fig. 7. Conceptual model of the climatic drivers and the related physical processes responsible for the hydroclimate anomalies observed in the northern tropical Americas between 600 and 1200 CE (adapted from Bhattacharya et al., 2017).

SST and LST, for the interval between 1860 and 2000 CE, provided evidence for the existence of a positive correlation between LST temperature anomalies in southern Central America and SSTs in the tropical North Atlantic and Pacific during the test period (Smith et al., 2008). The chironomid-inferred cooling at Lago Morrenas 3C, which began at ~610 CE, tracks the increasingly positive NAO index, which would drive decreasing SSTs in the western and southeastern Caribbean during this time (Figs. 6 and 7). Therefore, reduced SSTs in the tropical North Atlantic (negative AMO) may be a factor influencing hydroclimate conditions during the TCD and MCA in Costa Rica, and at other sites in the northern tropical Americas.

The paleoenvironmental record developed for Lago Morrenas 3C, together with the record previously reported for Laguna Zoncho, identify the existence of cool, dry conditions in mid- and high-elevation regions in Costa Rica between 610 and 1230 CE. The near absence of sub-fossil chironomid remains in the Zoncho core during this interval suggests that the decrease in effective moisture may have been greater here than in the highlands. Although depressed SSTs in the tropical Atlantic and a more southerly positioned ITCZ during the TCD-MCA interval would reduce rainfall across southern Central America, mid- and low-elevation sites on the Pacific slope can be more significantly affected. Additionally, if the southward penetration of the polar outbreaks and associated cold fronts are limited during the dry season, the intensity of the dry season would be amplified and strongly expressed at low to mid-elevations along the Pacific slope in Costa Rica. This may imply a higher vulnerability of hydrologic systems located at low to mid-elevations on the Pacific slope relative to the Atlantic slope of Costa Rica during intervals of severe drought when the mean annual position of ITCZ and/or the northernmost position of the ITCZ are located further south.

5. Conclusions

Analysis of sub-fossil chironomid remains from a sediment core recovered from Lago Morrenas 3C, a high-elevation glacial lake located in Chirripó NP, Costa Rica, documents the occurrence of notable faunal turnover between ~610 and 1230 CE. The change in the chironomid assemblage between ~610 and 1230 CE is inferred to reflect the onset of pronounced cooling, lower lake level, and a decrease in effective moisture. The existence of more positive $\delta^{13}C$ values between 700 and 1100 CE at Lago Morrenas 3C, which is inferred to reflect the expansion of *Muhlenbergia*, a C_4 grass with a preference for cold and dry habitats, supports the chironomid-based interpretation. Evidence for a severe drought at that time is also documented at Laguna Zoncho, a mid-elevation lake located on the Pacific slope of southern Costa Rica. These records together suggest that southern Central America was characterized by a relatively warmer and wet climate between 300 and 610 CE, intermediate temperatures and drier conditions between ~1230 and 1600 CE, and cold conditions between 1600 CE and present. These hydroclimate shifts in southern Central America between ~610 and 1230 CE generally overlap the MCA-TCD interval, and their timing supports the hypothesis that depressed SSTs, a stronger SLP gradient and NASH in the tropical North Atlantic, and a more southerly ITCZ position could account for the severe droughts in the tropical Americas from ~700 to 1100 CE.

Funding sources

This research was funded by a Provost's Summer Research Award from the University of Georgia (UGA) to David F. Porinchu, and research grants from the Geological Society of America, the Center for Archaeological Sciences and the Center for Applied Isotope Studies at UGA, and the crowdfunding platform Experiment.com to Jiaying Wu.

Acknowledgments

We thank José Luis Garita Romero for assistance in the field and Tom Maddox for providing guidance and conducting geochemical analyses at the Center of Applied Isotope Studies (CAIS at UGA). Appreciation is extended to Maarten Blaauw and Stephen Juggins for assistance in the use of multiple software and statistical packages and to Tripti Bhattacharya for sharing an early version of her paper on describing the mechanisms underlying pre-Medieval droughts in Mesoamerica.

References

Esquivel-Hernández, G., Sánchez-Murillo, R., Quesada-Román, A., Mosquera, G.M., Birkel, C., Boll, J., 2018. Insight into the stable isotopic composition of glacial lakes in a tropical alpine ecosystem: chirripó, Costa Rica. Hydrol. Process. 32 (24), 3588–3603.

Agar Cetin, A., 2014. Last 2000 Year Climate Sediment Record from the Belize Central Shelf Lagoon: A Detailed Archive of Droughts and Floods Linked to the Collapse of the Mayan Civilization and Caribbean Historical Famines. Doctoral dissertation, Rice University.

Aimers, J., Hodell, D., 2011. Societal collapse: drought and the Maya. Nature 479, 44–45.

Anchukaitis, K.J., Horn, S.P., 2005. A 2000-year reconstruction of forest disturbance from southern Pacific Costa Rica. Palaeogeogr. Palaeoclimatol. Palaeoecol. 221 (1–2), 35–54.

Bhattacharya, T., Byrne, R., Böhnel, H., Wogau, K., Kienel, U., Ingram, B.L., Zimmerman, S., 2015. Cultural implications of late Holocene climate change in the Cuenca Oriental, Mexico. In: Proceedings of the National Academy of Sciences *112* Pp, pp. 1693–1698.

Bhattacharya, T., Chiang, J.C., Cheng, W., 2017. Ocean-atmosphere dynamics linked to 800–1050 CE drying in Mesoamerica. Quat. Sci. Rev. 169, 263–277.

Bianchi, G.G., McCave, I.N., 1999. Holocene periodicity in North Atlantic climate and deep-ocean flow south of Iceland. Nature 397 (6719), 515.

Birks, H.J.B., Line, J.M., 1992. The use of rarefaction analysis for estimating palynological richness from Quaternary pollen-analytical data. Holocene 2 (1), 1–10.

Blaauw, M., Christen, J.A., 2011. Flexible paleoclimate age-depth models using an autoregressive gamma process. Bayesian analysis *6* (3), 457–474.

Bond, G., Showers, W., Cheseby, M., Lotti, R., Almasi, P., Priore, P., Cullen, H., Hajdas, I., Bonani, G., 1997. A pervasive millennial-scale cycle in North Atlantic Holocene and glacial climates. Science 278 (5341), 1257–1266.

Bond, R., Hajdas, I., Bonani, G., 2001. Persistent solar influence on North Atlantic climate during the Holocene. Science *294* (5549), 2130–2136.

Broccoli, A.J., Dahl, K.A., Stouffer, R.J., 2006. Response of the ITCZ to Northern Hemisphere cooling. Geophys. Res. Lett. 33 (1).

Brooks, S.J., Langdon, P.G., Heiri, O., Quaternary Research Association, 2007. The identification and use of palaearctic chironomidae larvae in palaeoecology. Quat. Res. Assoc. 1–274.

Chiang, J.C., Friedman, A.R., 2012. Extratropical cooling, interhemispheric thermal gradients, and tropical climate change. Annu. Rev. Earth Planet Sci. 40, 383–412.

Clawson, D.L., 1997. Latin America and the Caribbean. Wm. C. Brown Publishers.

Clement, R.M., Horn, S.P., 2001. Pre-Columbian land-use history in Costa Rica: a 3000-year record of forest clearance, agriculture and fires from Laguna Zoncho. Holocene 11, 419–426.

Coen, E., 1983. The Climate of Costa Rica. Chapter III of Costa Rica Natural History. University of Chicago, Illinois, USA.

Conroy, J.L., Overpeck, J.T., Cole, J.E., Shanahan, T.M., Steinitz-Kannan, M., 2008. Holocene changes in eastern tropical Pacific climate inferred from a Galápagos lake sediment record. Quat. Sci. Rev. 27 (11–12), 1166–1180.

Cook, E.R., Anchukaitis, K.J., Buckley, B.M., D'Arrigo, R.D., Jacoby, G.C., Wright, W.E., 2010. Asian monsoon failure and megadrought during the last millennium. Science 328 (5977), 486–489.

Cranston, P., 2010. http://chirokey.skullisland.info/.

Cubasch, U., Meehl, G.A., Boer, G.J., Stouffer, R.J., Dix, M., Noda, A., Senior, C.A., Raper, S., Yap, K.S., 2001. Projections of future climate change. In: Houghton, J.T., Ding, Y., Griggs, D.J., Noguer, M., Van der Linden, P.J., Dai, X., Maskell, K., Johnson, C.A. (Eds.), Climate Change 2001: the Scientific Basis: Contribution of Working Group I to the Third Assessment Report of the Intergovernmental Panel, pp. 526–582.

Curtis, J.H., Hodell, D.A., Brenner, M., 1996. Climate variability on the Yucatan peninsula (Mexico) during the past 3500 years, and implications for Maya cultural evolution. Quat. Res. 46, 37–47.

Diaz, H.F., Trigo, R., Hughes, M.K., Mann, M.E., Xoplaki, E., Barriopedro, D., 2011. Spatial and temporal characteristics of climate in medieval times revisited. Bull. Am. Meteorol. Soc. 92 (11), 1487–1500.

Diefendorf, A.F., Mueller, K.E., Wing, S.L., Koch, P.L., Freeman, K.H., 2010. Global

patterns in leaf 13C discrimination and implications for studies of past and future climate. Proc. Natl. Acad. Sci. Unit. States Am. *107* (13), 5738–5743.
Douglas, P.M., Pagani, M., Canuto, M.A., Brenner, M., Hodell, D.A., Eglinton, T.I., Curtis, J.H., 2015. Drought, agricultural adaptation, and sociopolitical collapse in the Maya lowlands. In: Proceedings of the National Academy of Sciences, vol. 112, pp. 5607–5612.
Douglas, P.M., Demarest, A.A., Brenner, M., Canuto, M.A., 2016. Impacts of climate change on the collapse of lowland Maya civilization. Annu. Rev. Earth Planet Sci. 44, 613–645.
Eggermont, H., Kennedy, D., Hasiotis, S.T., Verschuren, D., Cohen, A., 2008. Distribution of living larval chironomidae (insecta: Diptera) along a depth transect at kigoma bay, lake tanganyika: implications for palaeoenvironmental reconstruction. Afr. Entomol. 16, 162–184.
Enfield, D.B., Alfaro, E.J., 1999. The dependence of Caribbean rainfall on the interaction of the tropical Atlantic and Pacific Oceans. J. Clim. 12 (7), 2093–2103.
Epler, J., 1995. Identification Manual for the Larval Chironomidae (Diptera) of Florida. Identification Manual for the Larval Chironomidae (Diptera) of Florida.
Epler, J.H., 2001. Identification Manual for the Larval Chironomidae (Diptera) of North and South Carolina. John H. Epler, Crawford, South Carolina, pp. 1–526.
Fensterer, C., Scholz, D., Hoffmann, D., Spötl, C., Pajo_n, J.M., Mangini, A., 2012. Cuban stalagmite suggests relationship between Caribbean precipitation and the Atlantic multidecadal oscillation during the past 1.3 ka. Holocene 22, 1405–1412.
Figueroa-Rangel, B.L., Willis, K.J., Olvera-Vargas, M., 2008. 4200 Years of pine-pominated upland forest dynamics in west-central Mexico: human or natural legacy? Ecology 89, 1893–1907.
Fortin, M.C., Medeiros, A.S., Gajewski, K., Barley, E.M., Larocque-Tobler, I., Porinchu, D.F., Wilson, S.E., 2015. Chironomid-environment relations in northern North America. J. Paleolimnol. 54 (2–3), 223–237.
Giannini, A., Kushnir, Y., Cane, M.A., 2000. Interannual variability of Caribbean rainfall, ENSO, and the Atlantic ocean. J. Clim. 13 (2), 297–311.
Giorgi, F., Avissar, R., 1997. Representation of heterogeneity effects in earth system modeling: experience from land surface modeling. Rev. Geophys. 35 (4), 413–437.
Giorgi, F., Hewitson, B., Christensen, J., Hulme, M., Von Storch, H., Whetton, P., Jones, R., Mearns, L., Fu, C., Arritt, R., Bates, B., 2001. Regional Climate Information—Evaluation and Projections.
Glew, J.R., 1991. Miniature gravity corer for recovering short sediment cores. J. Paleolimnol. 5 (3), 285–287.
Gosse, H., Masson-Delmotte, V., Renssen, H., Delmotte, M., Fichefet, T., Morgan, V., Van Ommen, T., Khim, B.K., Stenni, B., 2004. A late Medieval warm period in the Southern Ocean as a delayed response to external forcing? Geophys. Res. Lett. 31 (6).
Graham, N., Ammann, C., Fleitmann, D., Cobb, K., Luterbacher, J., 2011. Support for global climate reorganization during the 'medieval climate anomaly. Clim. Dyn. 37, 1217–1245.
Haberyan, K.A., Horn, S.P., 2005. Diatom paleoecology of Laguna Zoncho, Costa Rica. J. Paleolimnol. *33* (3), 361–369.
Haberyan, K.A., Umaña, G.V., Collado, C., Horn, S.P., 1995. Observations on the plankton of some Costa Rican lakes. Hydrobiologia 312 (2), 75–85.
Haltia-Hovi, E., Saarinen, T., Kukkonen, M., 2007. A 2000-year record of solar forcing on varved lake sediment in eastern Finland. Quat. Sci. Rev. *26* (5–6), 678–689.
Haug, G.H., Günther, D., Peterson, L.C., Sigman, D.M., Hughen, K.A., Aeschlimann, B., 2003. Climate and the collapse of Maya civilization. Science 299 (5613), 1731–1735.
Heiri, O., Lotter, A.F., 2001. Effect of low count sums on quantitative environmental reconstructions: an example using sub-fossil chironomids. J. Paleolimnol. 26 (3), 343–350.
Hodell, D.A., Brenner, M., Curtis, J.H., Guilderson, T., 2001. Solar forcing of drought frequency in the Maya lowlands. Science 292 (5520), 1367–1370.
Hodell, D.A., Brenner, M., Curtis, J.H., 2005. Terminal classic drought in the northern Maya lowlands inferred from multiple sediment cores in Lake Chichancanab (Mexico). Quat. Sci. Rev. *24* (12–13), 1413–1427.
Hodell, D.A., Brenner, M., Curtis, J.H., 2007. Climate and cultural history of the northeastern Yucatan peninsula, Quintana roo, Mexico. Clim. Change 83 (1–2), 215–240.
Horn, S.P., 1993. Postglacial vegetation and fire history in Chirripó páramo of Costa Rica. Quat. Res. 40 (1), 107–116.
Horn, S.P., Kappelle, M., 2009. Fire in the páramo ecosystems of Central and South America. In: Cochrane, M.A. (Ed.), Tropical Fire Ecology. Tropical Fire Ecology-Springer Berlin Heidelberg, pp. 505–539.
Horn, S.P., Sanford Jr., R.L., 1992. Holocene fires in Costa Rica. Biotropica 354–361.
Horn, S.P., Orvis, K.H., Haberyan, K.A., 2005. Limnología de las lagunas glaciales en el páramo del Chirripó, Costa Rica. In: Páramos de Costa Rica. INBio Press, Santo Domingo de Heredia, Costa Rica, pp. 161–181.
Hughes, M.K., Diaz, H.F., 1994. Was there a 'medieval warm period', and if so, where and when? Clim. Change 26 (2–3), 109–142.
Hurrell, J.W., Deser, C., 2010. North Atlantic climate variability: the role of the north Atlantic oscillation. J. Mar. Syst. *79* (3–4), 231–244.
Jones, T.L., Brown, G.M., Raab, L.M., McVickar, J.L., Spaulding, W.G., Kennett, D.J., York, A., Walker, P.L., 1999. Environmental imperatives reconsidered: demographic crises in western North America during the medieval climatic anomaly. Curr. Anthropol. 40 (2), 137–170.
Juggins, S., 2003. C2 Program Version 1.4. Department of Geology, University of Newcastle, Newcastle upon Tyne, UK.
Juggins, S., Juggins, M.S., 2009. Package 'rioja'. *Analysis of quaternary science data*. Compr. R Arch. Netw.
Kappelle, M., 1991. Distribución altitudinal de la vegetación del Parque Nacional Chirripó, Costa Rica. Altitudinal distribution of vegetation at the Chirripo National Park, Costa Rica. *Brenesia., 36*, pp. 1–14.
Kappelle, M., Horn, S.P., 2016. The Páramo ecosystem of Costa Rica's highlands. In: Costa Rican Ecosystems. University of Chicago Press, pp. 492–523.
Keigwin, L.D., Boyle, E.A., 2000. Detecting Holocene changes in thermohaline circulation. Proc. Natl. Acad. Sci. Unit. States Am. 97 (4), 1343–1346.
Kennedy, L.M., Horn, S.P., 2008. A late Holocene pollen and charcoal record from La Selva Biological Station, Costa Rica. Biotropica 40 (1), 11–19.
Kennett, D.J., Breitenbach, S.F., Aquino, V.V., Asmerom, Y., Awe, J., Baldini, J.U., Bartlein, P., Culleton, B.J., Ebert, C., Jazwa, C., et al., 2012. Development and disintegration of Maya political systems in response to climate change. Science *338*, 788–791.
Kohn, M.J., 2010. Carbon isotope compositions of terrestrial C3 plants as indicators of (paleo) ecology and (paleo) climate. Proc. Natl. Acad. Sci. Unit. States Am. 107 (46), 19691–19695.
Lachniet, M.S., Seltzer, G.O., 2002. Late quaternary glaciation of Costa Rica. Geol. Soc. Am. Bull. *114* (5), 547–558.
Lachniet, M.S., Burns, S.J., Piperno, D.R., Asmerom, Y., Polyak, V.J., Moy, C.M., Christenson, K., 2004. A 1500-year el ninõ southern oscillation and rainfall history for the isthmus of Panama from speleothem calcite. J. Geophys. Res.: Atmosphere *109* (D20).
Lachniet, M.S., Bernal, J.P., Asmerom, Y., Polyak, V., Piperno, D., 2012. A 2400 yr Mesoamerican rainfall reconstruction links climate and cultural change. Geology *40* (3), 259–262.
Lachniet, M.S., Asmerom, Y., Polyak, V., Bernal, J.P., 2017. Two Millennia of Mesoamerican Monsoon Variability Driven by Pacific and Atlantic Synergistic Forcing. Quat. Sci. Rev. vol. *155*, 100–113.
Lane, C.S., Horn, S.P., 2013. Terrestrially derived n-alkane δD evidence of shifting Holocene paleohydrology in highland Costa Rica. Arctic Antarct. Alpine Res. *45*, 342–349.
Lane, C.S., Horn, S.P., Mora, C.I., 2004. Stable carbon isotope ratios in lake and swamp sediments as a proxy for prehistoric forest clearance and crop cultivation in the Neotropics. J. Paleolimnol. 32, 375–381.
Lane, C.S., Horn, S.P., Mora, C.I., Orvis, K.H., 2009. Late-Holocene paleoenvironmental change at mid-elevation on the Caribbean slope of the Cordillera Central, Dominican Republic: a multi-site, multi-proxy analysis. Quat. Sci. Rev. *28*, 2239–2260.
Lane, C.S., Horn, S.P., Mora, C.I., Orvis, K.H., Finkelstein, D.B., 2011a. Sedimentary stable carbon isotope evidence of late Quaternary vegetation and climate change in highland Costa Rica. J. Paleolimnol. 45, 323–338.
Lane, C.S., Horn, S.P., Orvis, K.H., Thomason, J.M., 2011b. Oxygen isotope evidence of Little ice age aridity on the Caribbean slope of the Cordillera Central, Dominican Republic. Quat. Res. 75 (3), 461–470.
Lane, C.S., Horn, S.P., Kerr, M.T., 2014. Beyond the Mayan lowlands: impacts of the terminal classic drought in the Caribbean Antilles. Quat. Sci. Rev. *86*, 89–98.
League, B.L., Horn, S.P., 2000. A 10000-year record of Páramo fires in Costa Rica. J. Trop. Ecol. 16 (5), 747–752.
Los, S.O., Collatz, G.J., Bounoua, L., Sellers, P.J., Tucker, C.J., 2001. Global interannual variations in sea surface temperature and land surface vegetation, air temperature, and precipitation. J. Clim. 14, 1535–1549.
Luteyn, J., 1999. Introduction to the páramo ecosystem. In: Luteyn, J.L. (Ed.), Páramos: A Checklist of Plant Diversity, Geographical Distribution, and Botanical Literature. The New York Botanical Garden Press, NY, pp. 1–39.
Luzzadder-Beach, S., Beach, T.P., Dunning, N.P., 2012. Wetland fields as mirrors of drought and the Maya abandonment. Proc. Natl. Acad. Sci. Unit. States Am. 109, 3646–3651.
Maldonado, T., Alfaro, E.J., Hidalgo, H.G., 2018. A review of the main drivers and variability of Central America's climate and seasonal forecast systems. Rev. Biol. Trop. 66 (1), 153–175.
Mann, M.E., Cane, M.A., Zebiak, S.E., Clement, A., 2005. Volcanic and solar forcing of the tropical Pacific over the past 1000 years. J. Clim. *18* (3), 447–456.
Mann, M.E., Zhang, Z., Hughes, M.K., Bradley, R.S., Miller, S.K., Rutherford, S., Ni, F., 2008. Proxy-based reconstructions of hemispheric and global surface temperature variations over the past two millennia. Proc. Natl. Acad. Sci. Unit. States Am. 105, 13252–13257.
Mann, M.E., Zhang, Z., Rutherford, S., et al., 2009. Global signatures and dynamical origins of the Little ice age and medieval climate anomaly. Science 326, 1256–1260.
Martinson, T.L., 1993. Physical environments of Latin America. In: Blouet, B.W., Blouet, O.M. (Eds.), Latin America and the Caribbean. John Wiley & Sons, New York, pp. 1–33.
Medina-Elizalde and, M., Rohling, E.J., 2012. Collapse of classic Maya civilization related to modest reduction in precipitation. Science 335 (6071), 956–959.
Medina-Elizalde, M., Burns, S.J., Lea, D.W., Asmerom, Y., von Gunten, L., Polyak, V., Vuille, M., Karmalkar, A., 2010. High-resolution stalagmite climate record from the Yucatan peninsula spanning the Maya terminal classic period. Earth Planet. Sci. Lett. 298, 255–262.
Mestas-Nuñez, A.M., Enfield, D.B., Zhang, C., 2007. Water vapor fluxes over the intra-Americas sea: seasonal and inter-annual variability and associations with rainfall. J. Clim. 20, 1910–1922.
Moy, C.M., Seltzer, G.O., Rodbell, D.T., Anderson, D.M., 2002. Variability of el niño/southern oscillation activity at millennial timescales during the Holocene

epoch. Nature 420 (6912), 162.
Olsen, J., Anderson, N.J., Knudsen, M.F., 2012. Variability of the north Atlantic oscillation over the past 5,200 years. Nat. Geosci. 5 (11), 808.
Orvis, K.H., Horn, S.P., 2000. Quaternary glaciers and climate on Cerro Chirripó, Costa Rica. Quat. Res. 54, 24–37.
Ouellette, G.R., 2013. Late Holocene Paleoenvironmental Reconstruction in Barbados.
Porinchu, D.F., MacDonald, G.M., 2003. The use and application of freshwater midges (Chironomidae: insecta: Diptera) in geographical research. Prog. Phys. Geogr. 27, 378–422.
Porinchu, D.F., Reinemann, S., Mark, B.G., Box, J.E., Rolland, N., 2010. Application of a midge-based inference model for air temperature reveals evidence of late-20th century warming in sub-alpine lakes in the central Great Basin, United States. Quat. Int. 215 (1–2), 15–26.
Potter, R., Li, Y.K., Horn, S.P., Orvis, K.H., 2019. Cosmogenic Cl-36 surface exposure dating of late Quaternary glacial events in the Cordillera de Talamanca, Costa Rica. Quat. Res. 1–16.
Pounds, J.A., Bustamante, M.R., Coloma, L.A., Consuegra, J.A., Fogden, M.P., Foster, P.N., La Marca, E., Masters, K.L., Merino-Viteri, A., Puschendorf, R., Ron, S.R., 2006. Widespread amphibian extinctions from epidemic disease driven by global warming. Nature 439, 161–167.
Radić, V., Bliss, A., Beedlow, A.C., Hock, R., Miles, E., Cogley, J.G., 2014. Regional and global projections of twenty-first century glacier mass changes in response to climate scenarios from global climate models. Clim. Dyn. 42 (1–2), 37–58.
Reimer, P.J., Bard, E., Bayliss, A., Beck, J.W., Blackwell, P.G., Ramsey, C.B., Buck, C.E., Cheng, H., Edwards, R.L., Friedrich, M., Grootes, P.M., 2013. IntCal13 and Marine13 radiocarbon age calibration curves 0–50,000 years cal BP. Radiocarbon 55 (4), 1869–1887.
Ridley, H., 2014. Recent Central American and Low Latitude Climate Variability Revealed Using Speleothem-Based Rainfall Proxy Records from Southern Belize. Doctoral dissertation, Durham University.
Rosenmeier, M.F., Hodell, D.A., Brenner, M., Curtis, J.H., Guilderson, T.P., Mar. 2002. A 4000-year lacustrine record of environmental change in the southern Maya lowlands, Peten, Guatemala. Quat. Res. 57, 183–190.
Sage, R.F., Wedin, D.A., Li, M., 1999. The biogeography of C4 photosynthesis: patterns and controlling factors. In: Sage, R.F., Monson, R.K. (Eds.), C4 Plant Biology. Academic Press, San Diego, pp. 313–374.
Schneider, T., Bischo, T., Haug, G.H., 2014. Migrations and dynamics of the intertropical convergence zone. Nature *513*, 45–53.
Schwarz, A.G., Redmann, R.E., 1988. C4 grasses from the boreal forest region of northwestern Canada. Can. J. Bot. 66 (12), 2424–2430.
Seager, R., Graham, N., Herweijer, C., Gordon, A.L., Kushnir, Y., Cook, E., 2007. Blueprints for medieval hydroclimate. Quat. Sci. Rev. 26 (19–21), 2322–2336.
Self, A.E., Brooks, S.J., Birks, H.J.B., Nazarova, L., Porinchu, D., Odland, A., Yang, H., Jones, V.J., 2011. The distribution and abundance of chironomids in high-latitude Eurasian lakes with respect to temperature and continentality: development and application of new chironomid-based climate-inference models in northern Russia. Quat. Sci. Rev. 30 (9–10), 1122–1141.
Smith, T.M., Reynolds, R.W., Peterson, T.C., Lawrimore, J., 2008. Improvements to NOAA's historical merged land–ocean surface temperature analysis (1880–2006). J. Clim. *21*, 2283–2296.
Sorey, L.C., 2014. Paleoclimatology and Paleotempestology Study of Blue Hole, Lighthouse Reef, Belize through Geochemical Proxies.
Spies, M., Andersen, T., Epler, J.H., Watson Jr., C.N., 2009. Chironomidae (non-biting midges). Man. Cent. Am. Diptera 1, 437–480.
Stansell, N.D., Steinman, B.A., Abbott, M.B., Rubinov, M., Roman-Lacayo, M., 2013. Lacustrine stable isotope record of precipitation changes in Nicaragua during the Little ice age and medieval climate anomaly. Geology 41, 151–154.
Taylor, M.A., Enfield, D.B., Chen, A.A., 2002. Influence of the tropical Atlantic versus the tropical Pacific on Caribbean rainfall. J. Geophys. Res.: Oceans 107 (C9).
Taylor, Z.P., Horn, S.P., Finkelstein, D.B., 2013a. Pre-hispanic agricultural decline prior to the Spanish conquest in southern Central America. Quat. Sci. Rev. 73, 196–200.
Taylor, Z.P., Horn, S.P., Finkelstein, D.B., 2013b. Maize pollen concentrations in Neotropical lake sediments as an indicator of the scale of prehistoric agriculture. Holocene 23, 78–84.
Taylor, Z.P., Horn, S.P., Finkelstein, D.B., 2015. Assessing intra-basin spatial variability in geochemical and isotopic signatures in the sediments of a small neotropical lake. J. Paleolimnol. 54 (4), 395–411.
Tedesco, K., Thunell, R., 2003. High-resolution tropical climate record for the last 6,000 years. Geophys. Res. Lett. *30* (17).
Ter Braak, C.J., Smilauer, P., 2002. CANOCO Reference Manual and CanoDraw for Windows User's Guide: Software for Canonical Community Ordination. http://www.canoco.com. version 4.5.
Turner, B.L., Sabloff, J.A., 2012. Classic period collapse of the central Maya lowlands: insights about human–environment relationships for sustainability. Proc. Natl. Acad. Sci. Unit. States Am. 309, 13908–13914.
Wagner, R.G., 1996. Mechanisms controlling variability of the interhemispheric sea surface temperature gradient in the tropical Atlantic. J. Clim. 9, 2010–2019.
Wahl, D., Estrada-Belli, F., Anderson, L., 2013. A 3400-year paleolimnological record of prehispanic human-environment interactions in the Holmul region of the southern Maya lowlands. Palaeogeogr. Palaeoclimatol. Palaeoecol. 379, 17–31.
Wahl, D., Byrne, R., Anderson, L., 2014. An 8700-year paleoclimate reconstruction from the southern Maya lowlands. Quat. Sci. Rev. 103, 19–25.
Walker, I.R., 2001. Midges; chironomidae and related Diptera. Dev. Paleoenviron. Res. *4*, 43–66.
Waylen, P.R., Caviedes, C.N., Quesada, M.E., 1996. Interannual variability of monthly precipitation in Costa Rica. J. Clim. 9 (10), 2606–2613.
Webster, J.W., Brook, G.A., Railsback, L.B., Cheng, H., Edwards, R.L., Alexander, C., Reeder, P.P., 2007. Stalagmite evidence from Belize indicating significant droughts at the time of pre-classic abandonment, the Maya hiatus, and the classic Maya collapse. Palaeogeogr. Palaeoclimatol. Palaeoecol. *250*, 1–17.
Weiss, H., Bradley, R.S., 2001. What drives societal collapse? Science 291, 609–610.
Wu, J., and Porinchu, D.F. *under review*. A High-Resolution Reconstruction of Late Holocene Fire Regimes in the Páramo of Chirripó National Park, Costa Rica: Evidence from Charcoal and Sediment Geochemistry. *Quaternary Research*.
Wu, J., Porinchu, D.F., Horn, S.P., Haberyan, K.A., 2015. The modern distribution of chironomid sub-fossils (Insecta: Diptera) in Costa Rica and the development of a regional chironomid-based temperature inference model. Hydrobiologia 742, 107–127.
Wu, J., Porinchu, D.F., Horn, S.P., 2017. A chironomid-based reconstruction of late-Holocene climate and environmental change for southern Pacific Costa Rica. Holocene 27, 73–84.
Wu, J., Porinchu, D.F., Campbell, N.L., Mordecai, T.M., Alden, E.C., 2019. Holocene hydroclimate and environmental change inferred from a high-resolution multi-proxy record from Lago Ditkebi, Chirripó National Park, Costa Rica. Palaeogeogr. Palaeoclimatol. Palaeoecol. *518*, 172–186.
Wunsch, O., Calvo, G., Willscher, B., Seyfried, H., 1999. Geologie der Alpinen Zone des Chirripó-Massives (Cordillera de Talamanca, Costa Rica, Mittelamerika). Profil *16*, 193–210.
Xie, S.P., Carton, J.A., 2004. Tropical Atlantic variability: patterns, mechanisms, and impacts. Earth climate: the ocean-atmosphere interaction. Geophys. Monogr 147, 121–142.